

RESEARCH

Open Access



# Salivary shield: *Rhodnius prolixus* salivary glandular extract reduces intestinal immunopathology and protects against *Toxoplasma gondii* infection

Roberto Augusto Pereira Sousa<sup>1</sup>, Jean Henrique Nunes de Paula<sup>2</sup>, Rafaela José Silva<sup>2</sup>, Samuel Cota Teixeira<sup>2</sup>, Flávia Batista Ferreira França<sup>2</sup>, Amanda Helena Leão Gonçalves<sup>1</sup>, Túlio Rodrigues Oliveira Silva<sup>1</sup>, Maria Julia Granero-Rosa<sup>1</sup>, Murilo Vieira Silva<sup>2</sup>, Marcos de Lucca Moreira Gomes<sup>1</sup>, Marcos Vinícius Silva<sup>1</sup>, Virmondos Rodrigues Junior<sup>1</sup>, José Roberto Mineo<sup>2</sup>, Bellisa Freitas Barbosa<sup>2</sup>, Eloisa Amália Vieira Ferro<sup>2</sup>, Carlo José Freire Oliveira<sup>1</sup> and Angelica Oliveira Gomes<sup>1\*</sup>

## Abstract

C57BL/6 mice, orally infected with *T. gondii*, experience pronounced severe intestinal inflammation, causing necrosis, weight loss, and bacterial translocation. In addition, immunomodulatory molecules such as lipocalins, nitrophorins, and apyrases are present in *R. prolixus* saliva. Our objective was to assess the immunomodulatory effects of the salivary gland extract (SGE) of *R. prolixus* in mice orally infected by *T. gondii*. Experimental groups received no treatment (PBS) or SGE (10 µg and 30 µg) in the chronic infection phase and (30 µg) in the acute infection phase. Control groups were non-infected and treated or not treated with SGE (30 µg). SGE was injected intraperitoneally daily, and mice were infected by gavage with 20 cysts of *T. gondii* (ME-49 strain) on the third treatment day. The treatment duration for the experiment was 23 days for the chronic infection phase (corresponding to 20 days of infection) and 12 days for the acute infection phase (corresponding to 9 days of infection). SGE-treated mice showed reduced small intestine shortening, weight loss, clinical scores, and higher survival rates. Treated mice also exhibited increased secretion of regulatory and protective cytokines (IL-4, IL-2, IL-10, IL-22) and higher levels of IL-4 (chronic phase), IL-2, and IL-22 (acute phase) in the gut. SGE treatment (30 µg) demonstrated protective effects in both the duodenum and ileum of *T. gondii*-infected mice. Treated animals showed better-preserved villus architecture, increased goblet and Paneth cell counts, and shallower crypts. Correlation data revealed that treated animals exhibited a more regulated and protective immune response. Overall, SGE contributed to the preservation of intestinal integrity and the reduction of inflammation. Thus, we conclude that SGE induces a regulatory response, mitigating inflammation and protecting against *T. gondii* infection.

**Keywords** Triatomines, Saliva, *Rhodnius prolixus*, Inflammatory bowel diseases, *Toxoplasma gondii*, Cytokines

\*Correspondence:

Angelica Oliveira Gomes  
angelica.gomes@uftm.edu.br

Full list of author information is available at the end of the article



© The Author(s) 2025. **Open Access** This article is licensed under a Creative Commons Attribution-NonCommercial-NoDerivatives 4.0 International License, which permits any non-commercial use, sharing, distribution and reproduction in any medium or format, as long as you give appropriate credit to the original author(s) and the source, provide a link to the Creative Commons licence, and indicate if you modified the licensed material. You do not have permission under this licence to share adapted material derived from this article or parts of it. The images or other third party material in this article are included in the article's Creative Commons licence, unless indicated otherwise in a credit line to the material. If material is not included in the article's Creative Commons licence and your intended use is not permitted by statutory regulation or exceeds the permitted use, you will need to obtain permission directly from the copyright holder. To view a copy of this licence, visit <http://creativecommons.org/licenses/by-nc-nd/4.0/>.

## Introduction

*Toxoplasma gondii*, an obligate intracellular parasite, causes Toxoplasmosis [1]. One of the reasons why this parasite is highly prevalent is because it interacts with and subverts host biological barriers [2].

The intestinal barrier is a semipermeable structure that allows the uptake of nutrients while simultaneously protecting hosts from pathogens. This barrier comprises many cells, mucus, bacteria, molecules, and proteins that maintain gut homeostasis [3]. The malfunction of gut structures, combined with environmental factors, pathogens, ethnic origin, or a dysregulated immune system, triggers inflammatory bowel disease (IBD). This condition is classified into two idiopathic disorders: Ulcerative Colitis and Crohn's Disease [4]. Crohn's disease is a transmural inflammation that primarily affects the ileum, colon, or both [5].

The C57BL/6 mouse model is highly susceptible to *Toxoplasma gondii* infection, making it a key system for studying the pathogenesis of toxoplasmosis and the host immune response. Oral infection with *T. gondii* in these mice induces intense mucosal inflammation resembling human Crohn's disease. This infection triggers a dysregulated inflammatory process that compromises intestinal barrier integrity, facilitating pathogen translocation and exacerbating inflammation [6]. The uncontrolled response can lead to severe complications such as sepsis, worsening symptoms, and potentially death. Despite their high susceptibility, the C57BL/6 mice provide a valuable model for analyzing immunopathological mechanisms and evaluating potential therapeutic interventions [7].

The damage caused by the parasite is mainly in the distal portion of the small intestine. Additionally, the disease in these mice is characterized histopathologically by transmural inflammation, fusion of villi cells, and increased necrosis. All these immunopathological processes are mediated by Th1 cells and cytokines, such as tumor necrosis factor- $\alpha$  (TNF- $\alpha$ ) and interferon- $\gamma$  (IFN- $\gamma$ ). In contrast, the IL-10 cytokine has an immunoregulatory role in preventing the damage triggered by *T. gondii* infection [8]. A previous study using an in vivo model of inflammatory bowel disease (IBD) demonstrated that Triatominae saliva effectively reduced the levels of the inflammatory cytokine IL-6 in the intestine [9].

Hematophagous insects have many strategies to modulate host hemostasis and inflammation. Consequently, the saliva of these insects contains vasodilators, inhibitors of the blood coagulation cascade, inhibitors of platelet aggregation, and immunomodulatory molecules. These substances are essential for obtaining an adequate blood meal and ensuring the survival of blood-sucking species [10].

*Rhodnius prolixus* is a hematophagous insect from the Reduviidae family, known as a vector of *Trypanosoma cruzi*, the causative agent of Chagas disease. The saliva of *R. prolixus* contains lipocalins, a family of proteins that interact with small molecules. Among these, Nitrophorin acts as an antihemostatic agent by releasing nitric oxide (NO) or histamine. Therefore, this protein family is crucial for anti-inflammatory and anti-hemostatic functions [11, 12].

Given their anti-inflammatory pharmacological properties, the saliva of these insects offers potential as a treatment for diseases involving cytokine imbalance, such as Crohn's disease and Toxoplasmosis. This study investigated the immunomodulatory effects of salivary gland extract (SGE) from *R. prolixus* in C57BL/6 mice orally infected with *T. gondii*.

## Material and methods

### Salivary gland extract (SGE)

*Rhodnius prolixus* males and females were obtained from the insect facility of the Federal University of Triângulo Mineiro (UFTM). A total of 280 insects were used for this experiment. The insects had their glands extracted after a 10 day fasting period, which allows for higher protein concentration. To prevent any batch differences from affecting the analysis, we pooled SGE from different batches before using them. The 280 insects used in the study were treated in the same manner to ensure consistency in the results.

Triatomines were housed in plastic jars (5.0 L or 3.2 L) sealed with fine mesh fabric and secured with elastic bands. Inside, a folded and perforated paper served as a support for feeding and shelter. Jars were placed on shelves lined with white paper, with oil traps at the base to prevent ants. Monthly cleaning involved transferring the insects to a tray, separating them by developmental stages, counting fifth-instar nymphs and adults, and replacing old paper. Dead insects and molts were discarded in 70% alcohol. For weekly feeding, mice were immobilized and placed over the insect jars for 1.5 h while monitoring. After feeding, confirmed by the insects' engorgement, the mice are untied and returned to their housing. Feeding details were recorded on the jar's label, as approved by the UFTM Animal Ethics Committee (23085.004370/2020-81). For salivary gland dissection, the triatomines were cleaned with distilled water and 70% ethanol. Subsequently, the head segment was separated, and the salivary gland was removed. The glands were ground using sterile needles (40  $\times$  1.6 mm, 16G), and the resulting material was centrifuged at 13000  $\times$  g. The supernatant salivary glandular extract (SGE) was collected, and protein concentration was measured using a NanoDrop 2000 spectrophotometer (Thermo Fisher

Scientific, Wilmington, DE, USA). Aliquots were stored at  $-80^{\circ}\text{C}$  until use.

### ***T. gondii* infection**

*Calomys callosus*, previously infected via oral gavage, were used to obtain *T. gondii* (ME49 strain) cysts. Following chronic infection, the brains of *C. callosus* were aseptically removed, washed, and then macerated. They were homogenized in 2 mL of sterile PBS (pH 7.2) using a 5 mL syringe and a 25×7 mm needle. The cysts were then counted under a light microscope and resuspended in a sterile PBS buffer to obtain a final concentration of 20 cysts per 100  $\mu\text{L}$  of PBS.

### **Animals**

Male C57BL/6 mice aged 6–8 weeks were housed in the animal facility of the Federal University of Uberlândia/Brazil (REBIR/UFU) under a 12 h light/dark cycle with ad libitum access to food and water. This study was approved by the Federal University of Uberlândia Animal Experimental Ethics Committee (CEUA/UFU) under protocol number 023/19. The C57BL/6 mice are highly susceptible to *T. gondii* infection, making them an essential model for studying the pathogenesis of toxoplasmosis and the immune response to this parasite.

Seven experimental groups were designed, each containing 10 mice: Non-infected and non-treated control; Non-infected and treated control (30  $\mu\text{g}$  of SGE); Chronic infection and non-treated; Chronic infection and treated (10  $\mu\text{g}$  of SGE or 30  $\mu\text{g}$  of SGE); Acute infection and treated (30  $\mu\text{g}$  of SGE); Acute infection and non-treated. The animals in the treated groups received SGE diluted in sterile PBS (phosphate-buffered saline), while untreated animals received only PBS. In this study, the untreated group, which received only PBS, serves as a baseline for comparison with the groups treated with SGE from *Rhodnius prolixus*. The administration of PBS mimics the injection procedure of the treated animals, but without the active compound (Fig. 1).

The experiment was designed for acute (9 days of infection and 12 days of treatment) and early Chronic phase of infection (20 days of infection and 23 days of treatment) based on literature and our previous experience [13, 14] (Fig. 1). The day euthanasia in the acute infection phase (9 days of infection and 12 days of treatment) was chosen because it was the first day of the acute phase that we observed a difference in weight loss between the treated and untreated groups. These data were obtained by daily following of animals from the chronic phase infection. The infection was performed on the 3rd day of treatment via oral gavage. The animals received 20 cysts diluted in sterile PBS, and non-infected controls received only PBS. The treatment was administered daily and performed

intraperitoneally using 10 or 30  $\mu\text{g}$  of SGE/day/animal). Body weight variation, clinical scores, and survival were evaluated daily for each mouse for a period of 23 days for chronic infection. The scores were determined according to BARTLEY et al. [15] with modifications (Fig. 1). Due to the lack of significant effects observed with the use of 10  $\mu\text{g}$  of SGE during the chronic phase of infection, we performed the acute phase of infection using only 30  $\mu\text{g}$  of SGE.

### **Euthanasia**

After 23 or 12 days from the beginning of the treatment, the animals were euthanized by cervical dislocation following intraperitoneal injection of ketamine (Syntec Brazil Ltd., SP, Brazil) and xylazine (Schering-Plough Coopers, Cotia, SP, Brazil). The small intestine was collected, and its length was measured. Then, small pieces of the intestine (approximately 1 cm from each segment) were collected for cytokine quantification using ELISA and Cytometric Bead Array (CBA) assays. Blood samples were collected through the retro-orbital collection.

### **Intestine measurement**

Small intestines were entirely removed, measured, and their shortening percentage calculated relative to uninfected mice according to Heimesaat et al. [16].

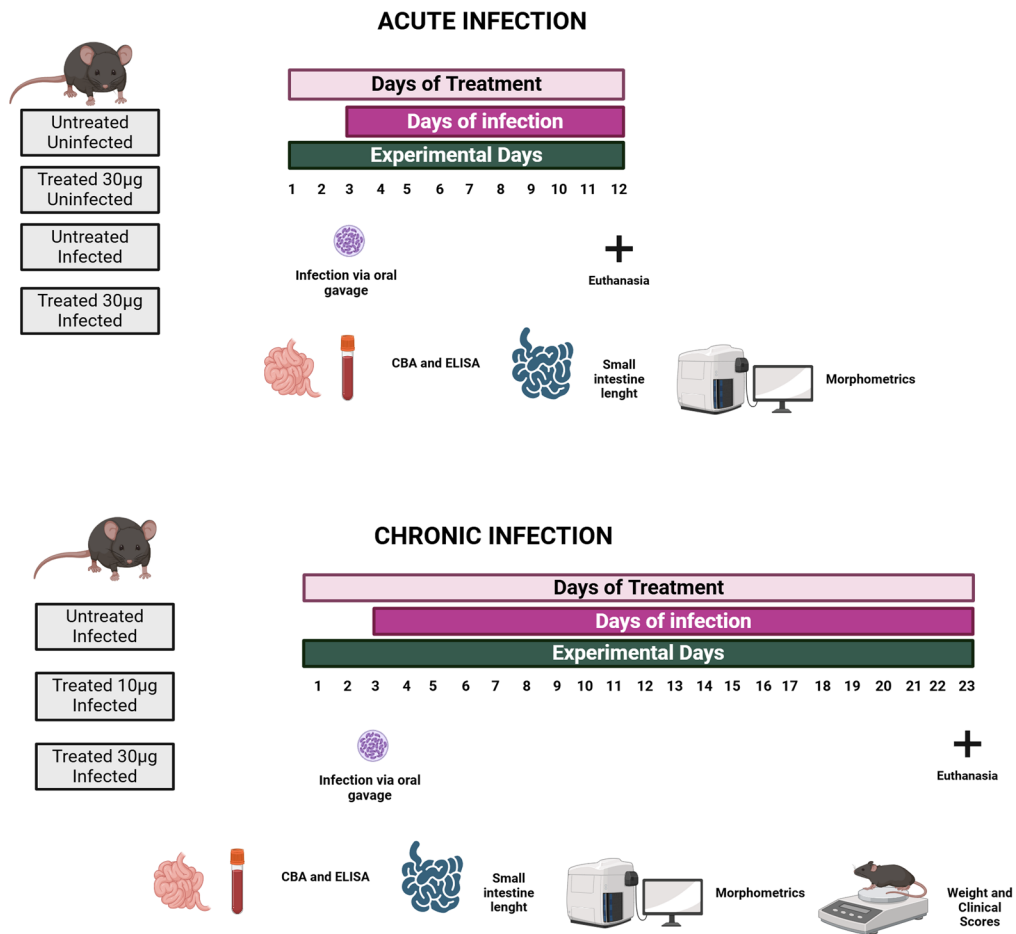
### **Histological preparation**

After collection, the small intestine was washed with PBS and segmented into the duodenum, proximal jejunum, distal jejunum, and ileum. The fragments were opened longitudinally, rolled with the mucosa facing outward, and subjected to the Swiss roll technique, enabling comprehensive histological analysis of the entire intestinal length [17]. Next, the intestinal fragments were fixed in 10% buffered formalin and dehydrated with increasing concentrations of ethyl alcohol. The clearing was performed by immersion in xylene and followed by paraffin infiltration. The four fragments were embedded in paraffin blocks, sectioned into 4  $\mu\text{m}$  slices using a Leica RM2125 RTS Rotary Microtome (Leica Biosystems, Buffalo Grove, IL, USA), and mounted on glass slides coated with Poly-L-Lysine (Sigma Aldrich), with two sections per slide spaced 40  $\mu\text{m}$ .

### **Morphometrics**

Histological sections of small intestine segments were analyzed. The tissue fragments were stained with the Periodic Acid-Schiff (PAS) reaction to detect mucins in goblet cells [18] and were counterstained with hematoxylin to highlight cell nuclei. The slides were digitized using the Leica Aperio AT Turbo ScanScope scanner (Leica Biosystems, Buffalo Grove, IL, USA), and image analysis

**A**



**B**

Faeces	Activity	Fur	Posture	Hidration
Normal (0pts)	Active (0pts)	Glossy (0pts)	Normal (0pts)	Normal (0pts)
Short (2 pts)	Hipoactive (1 pts)	Slightly Ruffled (1 pts)	Slightly Arched (1pts)	Slightly Dehydrated (1pts)
Absent (4 pts)	Motionless (2 pts)	Ruffled (2 pts)	Arched (2 pts)	Dehydrated (2 pts)
		Very Ruffled (4 pts)	Very Arched (4 pts)	Very Dehydrated (4 pts)

**Fig. 1 A** Experimental Design: Seven experimental groups were designed (10 animals/group): non-infected and non-treated control (injected with PBS); non-infected and treated control (30 µg of SGE); chronic infection and non-treated; chronic infection and treated (10 or 30 µg of SGE); Acute infection and treated (30 µg of SGE); acute infection and non-treated. The untreated control group received 100 µL of PBS, while the experimental groups received 10 or 30 µg of SGE daily via intraperitoneal injections. On the third day of treatment, infected mice were orally administered 20 cysts of *T. gondii* (ME 49 strain) through gavage. The experiment lasted 23 days for the chronic phase (23 days of treatment including 20 days of infection) and 12 days for the acute phase of infection (12 days of treatment including 9 days of infection). Throughout the experiment (23 days), daily recordings of weight and morbidity scores were registered. The euthanasia was conducted on the final day of treatment and the small intestine was measured and collected for morphometrics. Blood samples and small intestine fragments were obtained for cytokine measurement using CBA and ELISA. **B** The scores were determined according to BARTLEY et al. [15] with modifications

was conducted using Aperio ImageScope software (version 12.3.3).

For each section, 10 distinct fields were captured at 20× magnification, and the following measurements were taken using Image-Pro software (Media Cybernetics): villus length, crypt depth, villus area, epithelial area, connective tissue area, percentage of connective tissue, and goblet cell count. Measurements were obtained from 3 villi in each of the 10 fields captured per section, resulting in a total of 20 images per animal (10 per section). For each animal, the Swiss roll preparation was sectioned into two slides, spaced 40 μm apart.

To quantify villus connective tissue area, total villus area, villus epithelial area, and the percentage of connective tissue, 3 random villi were selected, and the respective areas were measured. The villus epithelial area was determined by subtracting the connective tissue area from the total villus area, providing an estimate of the epithelial area. Crypt length was measured from the base of the villi to the transition point between the epithelium and lamina propria. The percentage of villus connective tissue was calculated by dividing the connective tissue area by the total villus area and multiplying by 100. For goblet cell counts, the total number of epithelial cells in 3 randomly selected villi was measured, and goblet cells were quantified per 1000 μm<sup>2</sup> of epithelium. For Paneth cell quantification, 3 random crypts were selected per image, and 10 images were analyzed.

### Cytokines quantification

For the quantification of local cytokines, fragments of the duodenum, jejunum, and ileum were weighed and homogenized in radioimmunoprecipitation assay buffer, supplemented with protease inhibitor tablets (Roche Diagnostics GmbH, Mannheim, Germany). The solution's volume was adjusted to achieve a tissue concentration of 200 mg/mL during homogenization. The homogenates were centrifuged at high speed, and the supernatant was collected for cytokine measurement using ELISA and CBA assays. In addition, serum samples were used to quantify cytokines.

Cytokine profiles were measured using the CBA mouse kit (BD Bioscience, San Diego, CA, United States) following the manufacturer's instructions. The samples were analyzed using BD™ flow cytometry (FACSCanto, BD Company, San Diego, CA, United States), and the data were recorded using BD™ Cell Quest software. Cytokine levels were expressed as pg per 10 mg of small intestine extract. Cytokines such as IL-23, IL-12, IL-4, IL-6, IL-10 (BD OptEIA™), and MIF, TGF-β, IL-22, IL-5, and IL-17 (R&D Systems, Inc.) were quantified in intestinal tissue, while IL-22, IL-5, MIF, and TGF-β were also measured in

serum samples. The ELISA was performed according to the manufacturer's instructions, and the concentration of each cytokine was determined by extrapolating curves with known concentrations for each cytokine.

### Statistical analyses

Data analysis was conducted using GraphPad Prism software (version 8.0, GraphPad Software Inc., San Diego, CA, USA). Results were expressed as mean ± standard deviation (SD) with 10 animals per group (n=10). Statistical comparisons between experimental groups were performed using one-way ANOVA followed by Sidak's post-test. Two-way ANOVA was used to evaluate the simultaneous effects of two independent variables, followed by Tukey's post-test to identify specific differences between groups. Correlation matrices were calculated in R Studio. Spearman's test was used for non-parametric data, while Pearson's test was applied for parametric data. Heatmaps were generated using the corrplot package (v0.94; Wei & Simko, 2024). Correlation matrix data were exported to Cytoscape software (version 3.8.2) and analyzed using the MetScape package. This tool enables the construction and visualization of correlation networks. For network visualization, only correlation values greater than 0.5 or less than -0.5 were considered.

## Results

### Animals treated with *R. prolixus* SGE exhibited fewer clinical manifestations than non-treated ones

Daily clinical score assessments were conducted in the chronic phase group to evaluate the potential of *R. prolixus* SGE in reducing clinical signs of toxoplasmosis. Thus, animals treated with 10 μg or 30 μg of SGE and non-treated mice were evaluated daily. No clinical symptoms were observed in any group until the 8th day of treatment (5th day of infection). From the 9th to the 13th day of treatment (6th to 10th day of infection), animals developed acute disease symptoms, but no significant differences were observed between groups. The 30 μg SGE-treated group exhibited significantly lower clinical scores than the non-treated group on 14th, 16th to 18th, 20th, 22nd, and 23rd treatment days (11st, 13th to 15th, 17th, 19th, and 20th days of infection). Additionally, the 30 μg SGE group showed significantly lower scores than the 10 μg group on days 16, 17, 20, 21, and 22 of the treatment (Fig. 2A). Analysis of overall scores indicated that animals treated with 30 μg of SGE showed fewer clinical manifestations compared to both the non-treated group and the 10 μg SGE group (Fig. 2B). These findings suggest that treatment with 30 μg of *R. prolixus* SGE reduced clinical scores, highlighting its potential to alleviate the clinical signs of intestinal toxoplasmosis.

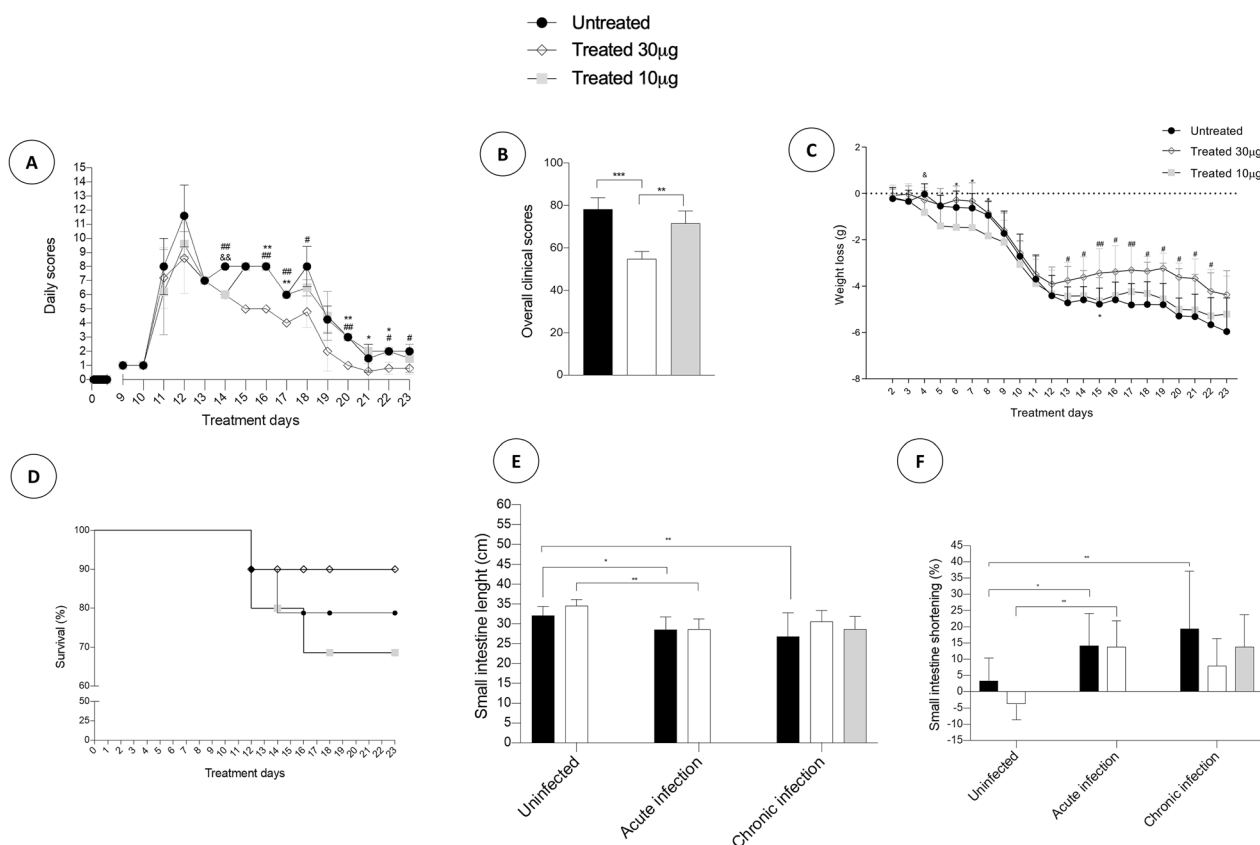


**Fig. 2** Clinical outcomes in C57BL/6 infected mice untreated or treated with SGE (10 or 30 µg). **A** Clinical scores were assessed daily over the 23-day treatment period. **B** Overall clinical scores; **C** The percentage of weight loss; **D** Survival rates measurements. Differences in daily scores, daily loss percentage weight, and overall score analysis were analyzed using one-way ANOVA. Significant variations were indicated as follows: asterisks (\*) indicate comparisons between treated animals 10 µg and 30 µg (\* p ≤ 0.05, \*\* p ≤ 0.01, \*\*\* p ≤ 0.001); Hashtag (#) indicate comparisons between untreated and treated animals (SGE 30 µg), (# p ≤ 0.05, ## p ≤ 0.01, ### p ≤ 0.001); Ampersand (&) indicate comparisons between untreated and treated animals (SGE 10 µg) (p ≤ 0.05, && indicates p ≤ 0.01, &&& indicates p ≤ 0.001). Small intestine length in C57BL/6 mice infected or not with *T. gondii* and treated or not with SGE (10 µg or 30 µg) during chronic or acute phases. **E** Represents the measured length of the small intestine. Data were analyzed using 2-way ANOVA followed by Tukey’s multiple comparison post-test. **F** Illustrates the percentage of shortening Asterisks indicated statistical significance, \* p ≤ 0.05 and \*\* p ≤ 0.01 (n = 10 mice per group)

**R. prolixus** SGE has a protective effect against weight loss during toxoplasmosis

Daily weight assessments were performed in the chronic phase group to evaluate whether SGE treatment could protect mice from weight loss. Mice experienced weight loss from the 5th to the 12th day of treatment (2nd to the 9th day of infection). On the 9th day of infection/12th day of treatment, the first distinction between treated (30 µg) and non-treated groups was observed (Fig. 2C). Despite no statistical difference, this parameter was used to choose the euthanasia date in the acute phase of infection (Fig. 1A). By the 13th to 22th day of treatment (10th to 19th day of infection), groups treated with 30 µg of *R. prolixus* saliva showed significant differences compared to the non-treated group. Additionally, the 30 µg SGE group showed significantly lower scores than the 10 µg

group on day 16th of treatment (13th day of infection) (Fig. 2C).

**Animals treated with R. prolixus SGE showed a higher survival rate**

The survival rate was calculated to evaluate the potential protective effect of SGE on mouse mortality. We analyzed the survival rates of mice treated with 10 or 30 µg of SGE compared to non-treated animals. Our results revealed that animals treated with 30 µg of SGE (90%) have had a higher survival rate compared to the 10 µg SGE group (68%) and the non-treated group (79%). However, no significant difference was observed among the groups (Fig. 2D).

### Animals treated with *R. prolixus* SGE showed less small intestine shortening during the chronic phase of toxoplasmosis

We measured the length of the intestine after euthanasia to determine if SGE could protect against intestinal shortening. Our results demonstrated that untreated animals exhibited a shorter intestine and a higher percentage of intestine shortening compared to animals in both the acute and chronic phases of infection. Furthermore, treated animals receiving 30  $\mu$ g of SGE showed a smaller intestine length and a higher percentage of intestine shortening compared to those in the acute phase of infection (Fig. 2E and F).

### *Rhodnius prolixus* SGE modulated systemic cytokines during *Toxoplasma gondii* infection

Cytokine profiles were analyzed to assess the influence of SGE on modulating the systemic immune response

during both the acute and chronic phases of infection. Our goal was to determine whether treatment with SGE could elicit an immune response capable of restricting *T. gondii* immunopathology.

Regarding Th1 cytokines, our data have demonstrated that systemic inflammatory cytokines (TNF, IFN- $\gamma$ , and MIF) have been increased in response to *T. gondii* infection in both the acute and chronic phases (Fig. 3A–C). Comparisons between untreated and treated mice revealed that during the acute phase of infection, TNF secretion was higher in treated mice compared to non-treated ones (Fig. 3A). No significant differences between untreated and treated mice were detected for the other cytokines analyzed. Additionally, we observed a significant decrease in inflammatory cytokines (TNF and IFN- $\gamma$ ) during the transition from the acute to the chronic phase of infection in both groups, treated and untreated (Fig. 3A and B). For MIF, *T. gondii* infection triggered an

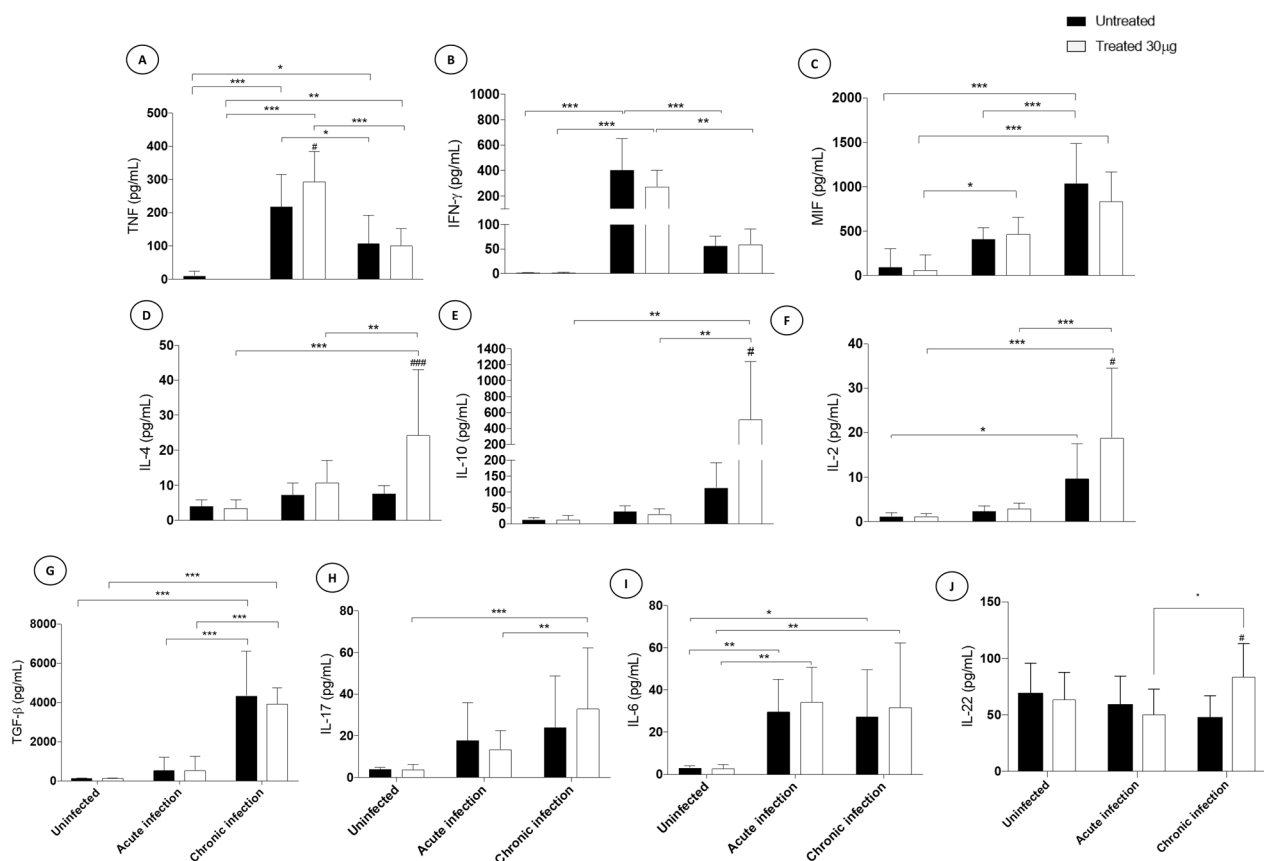


**Fig. 3** Systemic cytokines were analyzed using CBA and ELISA in C57BL/6 mice, whether infected or not with *T. gondii*, and treated or not with SGE (30  $\mu$ g) during chronic or acute infection phases. The cytokines were measured in mice serum, and data are expressed as the mean and standard deviation of cytokine secretion (pg/mL). **A** TNF, **B** IFN- $\gamma$ , **C** MIF, **D** IL-4, **E** IL-10, **F** IL-2, **G** TGF- $\beta$ , **H** IL-17, and **I** IL-6. # Represents significant differences between treated and untreated groups in the same experimental condition (treated and untreated mice). \*Represents differences between different experimental conditions (uninfected, acute infection, and chronic infection). Tests were performed using 2-way ANOVA followed by Tukey's multiple comparison post-test, and differences were considered significant when \* = 0.05, \*\* = 0.01, \*\*\* = 0.001. # = 0.05, ## = 0.01, ### = 0.001 (n = 10 mice per group). IFN- $\gamma$ , TNF, IL-17, IL-6, IL-4, IL-2, and IL-10 were measured by CBA, and MIF and TGF- $\beta$  were measured by ELISA

increase in this cytokine's level during both the acute and chronic infection phases in treated mice and during the chronic phase in untreated mice. Notably, MIF secretion was higher during the chronic phase compared to the acute phase for untreated animals (Fig. 3C).

Regarding Th2/Treg cytokines, our results showed that serum anti-inflammatory cytokines were elevated in response to *T. gondii* infection in the chronic phase for both treated (IL-4, IL-10, IL-2, and TGF- $\beta$ ) and untreated (IL-2 and TGF- $\beta$ ) animals (Fig. 3D–G). Comparisons between untreated and treated mice revealed that during the chronic phase of infection, IL-4, IL-10, and IL-2 secretion were higher in treated mice compared to non-treated ones (Fig. 3D–F). A significant increase in anti-inflammatory cytokines was observed during the transition from the acute to the chronic phase of infection in both treated (IL-4, IL-10, IL-2, and TGF- $\beta$ ) and untreated (TGF- $\beta$ ) groups (Fig. 3D–H).

Regarding systemic Th17 responses, our data revealed that treated mice exhibited a significant increase in IL-17 secretion in response to infection during the chronic phase. Furthermore, IL-17 secretion was elevated in treated mice during the transition from the acute to chronic phase of infection (Fig. 3H). Additionally, IL-6 levels increased in response to *T. gondii* infection in both the acute and chronic phases for treated and untreated mice (Fig. 3I). Finally, systemic IL-22 was significantly higher in treated animals during the acute phase compared to treated animals in the chronic phase. During the chronic phase, treated and infected animals had significantly higher serum levels of IL-22 than untreated and infected animals (Fig. 3J).

#### ***Rhodnius prolixus* SGE modulated intestinal cytokines in response to *T. gondii* infection**

This study investigated the impact of *T. gondii* infection on intestinal cytokine profiles. The results revealed that *T. gondii* infection significantly increased the production of intestinal TNF and IFN- $\gamma$  during the acute phase of infection in both treated and non-treated groups compared to uninfected mice. However, the production of these cytokines decreased during the transition from the acute to the chronic phase of infection. Results were statistically significant for the treated group (TNF) or for both the treated and untreated groups (IFN- $\gamma$ ) (Fig. 4A, B). The levels of intestinal IL-12 were significantly higher in treated mice during the acute phase of infection compared to uninfected treated ones (Fig. 4C).

Intestinal IL-5 levels were significantly increased during the acute phase of infection in both treated and untreated mice compared to uninfected controls. Moreover, IL-5 levels were significantly reduced during the transition from the acute to the chronic phase of infection for both

treated and untreated mice (Fig. 4D). Regarding IL-2, treated animals produced significantly more IL-2 than non-treated animals during the acute phase of infection (Fig. 4E). Additionally, for treated mice, IL-2 and TGF- $\beta$  levels were significantly lower in the chronic infection phase compared to the acute infection phase or compared to uninfected mice (Fig. 4E and F, respectively). Concerning IL-4, production was increased due to SGE treatment during the chronic infection phase. IL-4 production in treated mice was significantly higher in the chronic phase of infection compared to both the acute infection phase and uninfected controls (Fig. 4G). For IL-10, no significant differences were observed between the groups (Fig. 4H). For MIF, uninfected and untreated mice produced more MIF than to infected mice during both the acute and chronic infection phases. Likewise, MIF production in the chronic infection phase of treated mice was reduced compared to uninfected mice or the acute infection phase (Fig. 4I).

Regarding intestinal Th17 cytokines, IL-17 production significantly decreased in treated infected groups during both the acute and chronic phases compared to uninfected controls (Fig. 4J). IL-6 production was significantly increased during the acute infection phase in treated mice. The transition from the acute to chronic infection phase caused a decrease in IL-6 production, with this decrease being significant for untreated mice (Fig. 4K). During the acute infection phase, treated mice produced significantly more IL-22 than non-treated mice. In the treated group, IL-22 production was significantly higher in the acute infection phase compared to both uninfected mice and the chronic phase of infection (Fig. 4L). Finally, IL-23 production during the acute phase was significantly lower in treated mice compared to non-treated ones. In contrast, during the chronic infection phase, IL-23 levels were significantly higher in treated mice compared to untreated ones. In treated mice, acute infection caused a decrease in IL-23 production, while the chronic infection phase triggered an increase in IL-23 compared to uninfected controls. The transition from the acute to chronic infection phase caused an increase in IL-23 production (Fig. 4M).

#### **SGE has protective effects against pathology in the duodenum**

To evaluate the protective role of SGE against intestinal pathology, we analyzed various morphometric parameters in the duodenum, including the count of goblet cells and Paneth cells. The groups treated with 30  $\mu$ g in the chronic phase showed a significantly larger villus area, villi connective tissue, epithelium area, and villus length compared to the acute phase treated group and the uninfected treated group. Additionally, in the chronic phase,

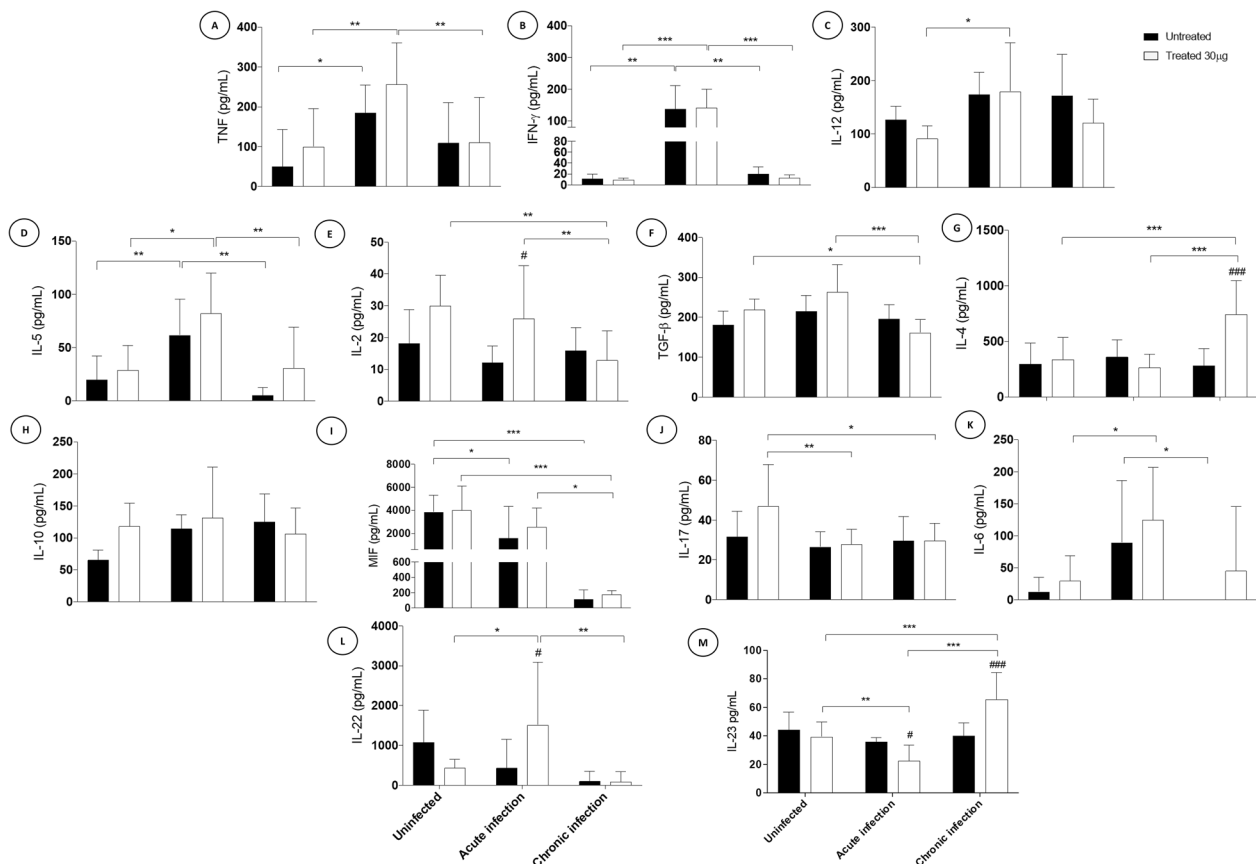


**Fig. 4** Intestinal cytokines were analyzed using CBA and ELISA in C57BL/6 mice, whether infected or not with *T. gondii*, and treated or not with SGE (30 µg) during chronic or acute infection phases. Fragments of the small intestine were collected and homogenized in RIPA buffer and adjusted to a concentration of 200 mg/mL. Data are expressed as the mean and standard deviation of cytokine amounts. **A** TNF, **B** IFN-γ, **C** MIF, **D** IL-5, **E** IL-2, **F** IL-2, **G** TGF-β, **H** IL-17, and **I** IL-6. # Represents significant differences between treated and untreated groups in the same experimental condition (treated and untreated mice). \*Represents differences between different experimental conditions (uninfected, acute infection, and chronic infection). Tests were performed using 2-way ANOVA followed by Tukey's multiple comparison post-test, and differences were considered significant when \* = 0.05, \*\* = 0.01, \*\*\* = 0.001. # = 0.05, ## = 0.01, ### = 0.001 (n = 10 mice per group). IFN-γ, TNF, IL-17, IL-6, IL-4, IL-2, and IL-10 were measured by CBA, whereas IL-12, MIF, IL-5, TGF-β, IL-22, and IL-23 were measured by ELISA

treatment with SGE (30 µg) resulted in a larger intestinal epithelial area than untreated animals (Fig. 5A–D).

Infected animals treated with SGE in the acute phase exhibited the highest number of goblet cells, surpassing those treated with SGE in the chronic phase and uninfected mice. Additionally, infected, untreated animals in the chronic phase had fewer goblet cells than untreated animals in the acute phase and uninfected, untreated animals. In the acute phase, treatment with SGE significantly increased goblet cell count compared to untreated animals (Fig. 5E). Our data showed that, the percentage of connective tissue was higher in chronic infection phase compared to acute phase in both, treated and non-treated mice. Also, in non-treated mice, the percentage of connective tissue is higher in chronic infection phase than in non-infected mice (Fig. 5F). Our results demonstrated that *T. gondii* infection leads to an increase in

intestinal crypts, with a more pronounced effect in the chronic phase. Infected animals treated with SGE 30 µg, in both the acute and chronic phases, exhibited shallower crypts compared to their respective untreated groups (Fig. 5G). Our results also demonstrated that *T. gondii* infection has led to a depletion in the Paneth cells. However, a recovery in this number was observed in the chronic phase. Finally, animals treated with SGE in the chronic phase showed a significantly higher number of Paneth cells compared to untreated animals in the chronic and acute phases (Fig. 5H). In general, histological analysis showed that uninfected mice maintained preserved intestinal architecture. In contrast, infected, untreated animals in the acute phase displayed larger crypts, fewer goblet cells and slightly enlarged villi due to the accumulation of subepithelial edema. Infected animals treated with SGE in the acute phase exhibited

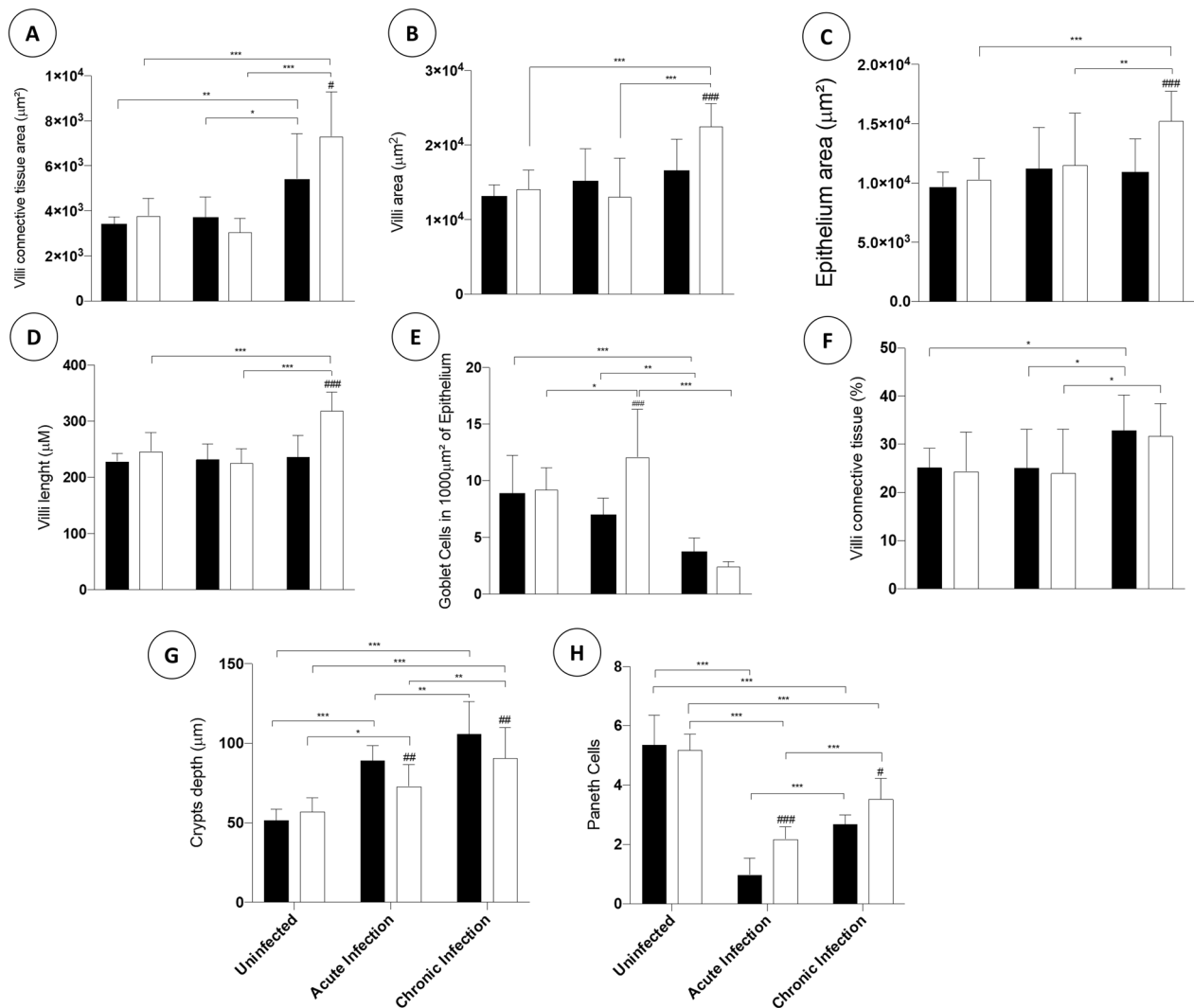


**Fig. 5** Morphometric study of the duodenum in C57BL/6 mice, infected or not with *T. gondii* and treated or not with SGE (30  $\mu\text{g}$ ) during the chronic or acute phases. # Represents significant differences between groups in the same phase of the disease. \* Represents differences between different experimental conditions (uninfected, acute infection, and chronic infection). Tests were performed using two-way ANOVA followed by Tukey's multiple comparison post-test, and differences were considered significant when \*  $\leq 0.05$ , \*\*  $\leq 0.01$ , \*\*\*  $\leq 0.001$ . #  $\leq 0.05$ , ##  $\leq 0.01$ , ###  $\leq 0.001$  (n = 10 mice per group)

smaller crypts and more significant number of goblet and Paneth cells (Fig. 6A–D).

In the chronic infection phase, animals treated with SGE showed significantly larger villus area, greater connective tissue area, longer villus length, shallower crypts, and a higher number of Paneth cells compared to untreated animals. Subepithelial edema was mainly observed in the untreated groups. (Fig. 6E–F). Image analysis revealed that uninfected animals preserved Paneth cells. Infected animals in the acute phase showed a depletion in the number of Paneth cells. However, treatment with SGE in the acute phase significantly increased the number of these cells (Fig. 7A–D). In the chronic

phase, a recovery in the number of Paneth cells was observed in all groups. However, animals treated with SGE showed a significantly higher number of these cells compared to untreated animals (Fig. 7E–G). Overall, the results indicate a protective effect of SGE on intestinal integrity, especially in the chronic phase of the pathology.

#### SGE has protective effects against pathology in the ileum

Various morphometric parameters were observed in the ileum to assess the protective role of SGE against intestinal pathology, including goblet cell and Paneth cell counts. In the acute phase, animals treated with SGE showed a decrease in villus area compared to uninfected

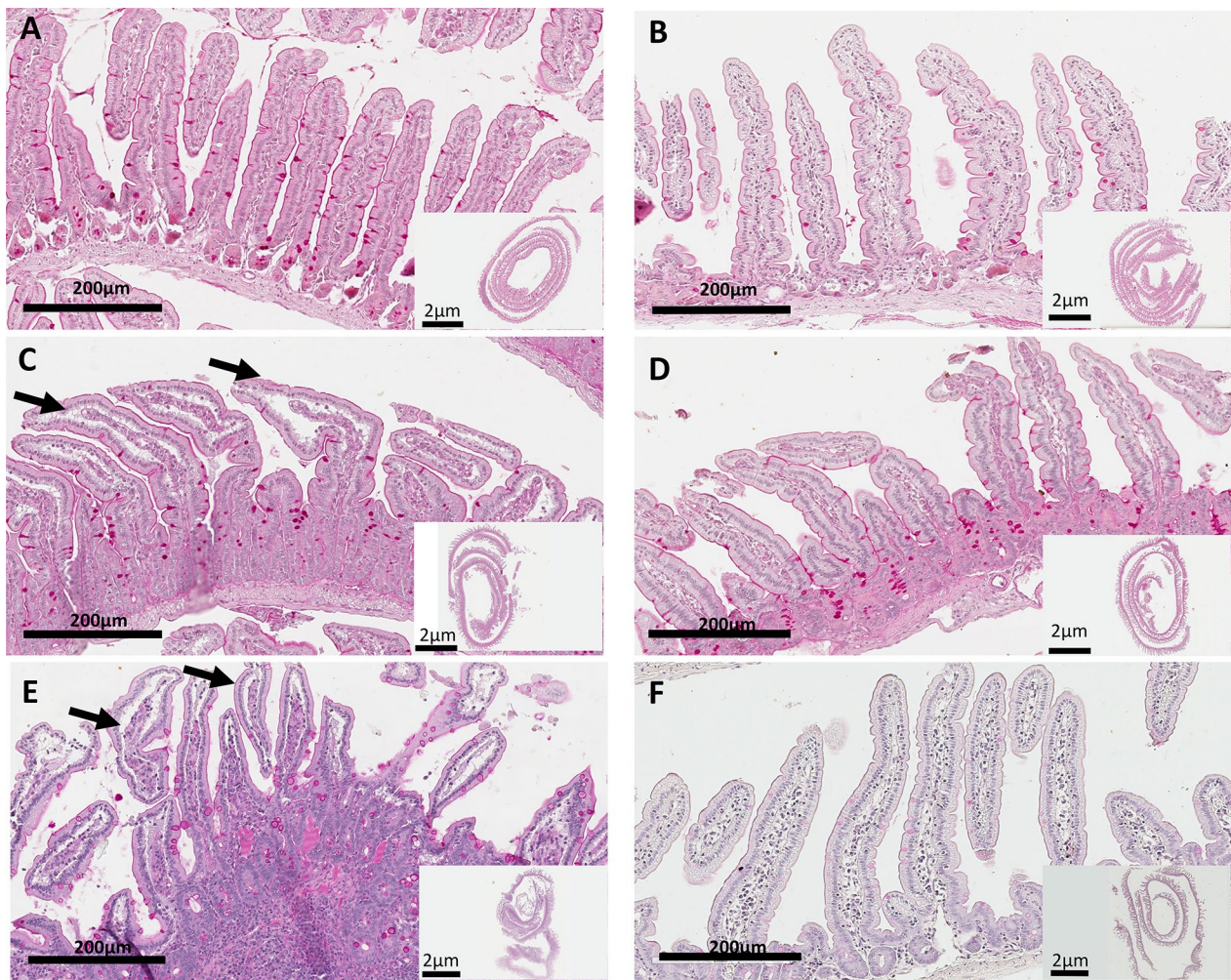


**Fig. 6** Duodenum of C57BL/6 mice, infected or not with *T. gondii* and treated or not with SGE 30 µg during the chronic or acute phases. Tissue sections of 4 µm, embedded in paraffin, were stained with Periodic Acid-Schiff (PAS). The slides were scanned, and images were captured using Aperio Imagescope software (version 12.3.3). Original magnification: 20x. Arrows indicate subepithelial edema. The scale bar represents 200 µm for a 20 × magnification of the epithelium or 2 µm for a 2 × magnification of a Swiss roll. The categories represented are: **A** Uninfected, untreated animals; **B** Uninfected animals treated with SGE 30 µg; **C** Infected, untreated animals in the acute phase; **D** Infected animals treated with SGE 30 µg in the acute phase; **E** Infected, untreated animals in the chronic phase; **F** Infected animals treated with SGE 30 µg in the chronic phase

treated animals. The chronic phase of the disease led to an increase in the villus area compared to animals in the acute phase or the control group. In the acute phase, untreated animals exhibited a larger villus area compared to those treated with SGE. Conversely, in the chronic phase, animals treated with SGE had the largest villus area (Fig. 8A).

Our data demonstrated that *T. gondii* infection caused a significant increase in connective tissue in the chronic phase of infection in treated and non-treated mice. Also, connective tissue in the chronic phase is higher than in the acute infection phase. Moreover, untreated animals in the acute phase showed more villi connective tissue compared to SGE-treated mice (Fig. 8B). In the acute

infection phase, animals treated with SGE had a reduced epithelial area of the villi compared to uninfected, treated animals. Moreover, infection led to a significant increase in epithelial area during the chronic phase compared to control and acute phase animals (Fig. 8C). During the acute phase, animals treated with SGE showed a reduction in villus length compared to uninfected, treated animals. Additionally, *T. gondii* infection significantly increased villus length during the chronic phase compared to control and acute phase animals. In the acute infection phase, untreated animals exhibited higher villi length than SGE-treated mice (Fig. 8D). Our results indicated that chronic phase infection caused a significant reduction in goblet cells compared to uninfected

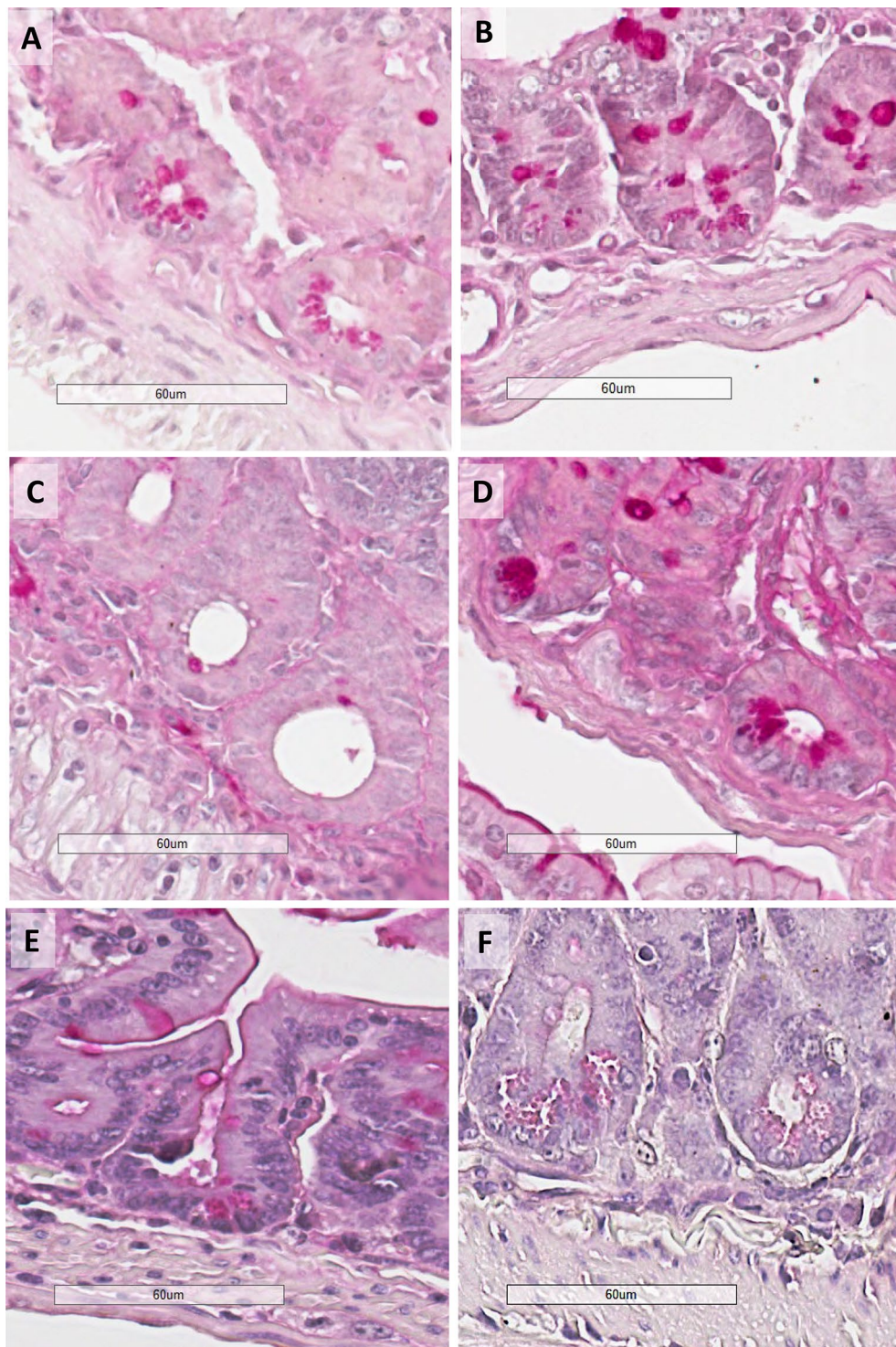


**Fig. 7** Paneth cells in the duodenum of C57BL/6 mice, infected or not with *T. gondii* and treated or not with SGE 30 μg during the chronic or acute phases. Tissue sections of 4 μm, embedded in paraffin, were stained with Periodic Acid-Schiff (PAS). The slides were scanned, and images were captured using Aperio Imagescope software (version 12.3.3). Original magnification: 40x. Scale bar = 60 μm. The categories represented are: **A** Uninfected, untreated animals; **B** Uninfected animals treated with SGE 30 μg; **C** Infected, untreated animals in the acute phase; **D** Infected animals treated with SGE 30 μg in the acute phase; **E** Infected, untreated animals in the chronic phase; **F** Infected animals treated with SGE 30 μg in the chronic phase

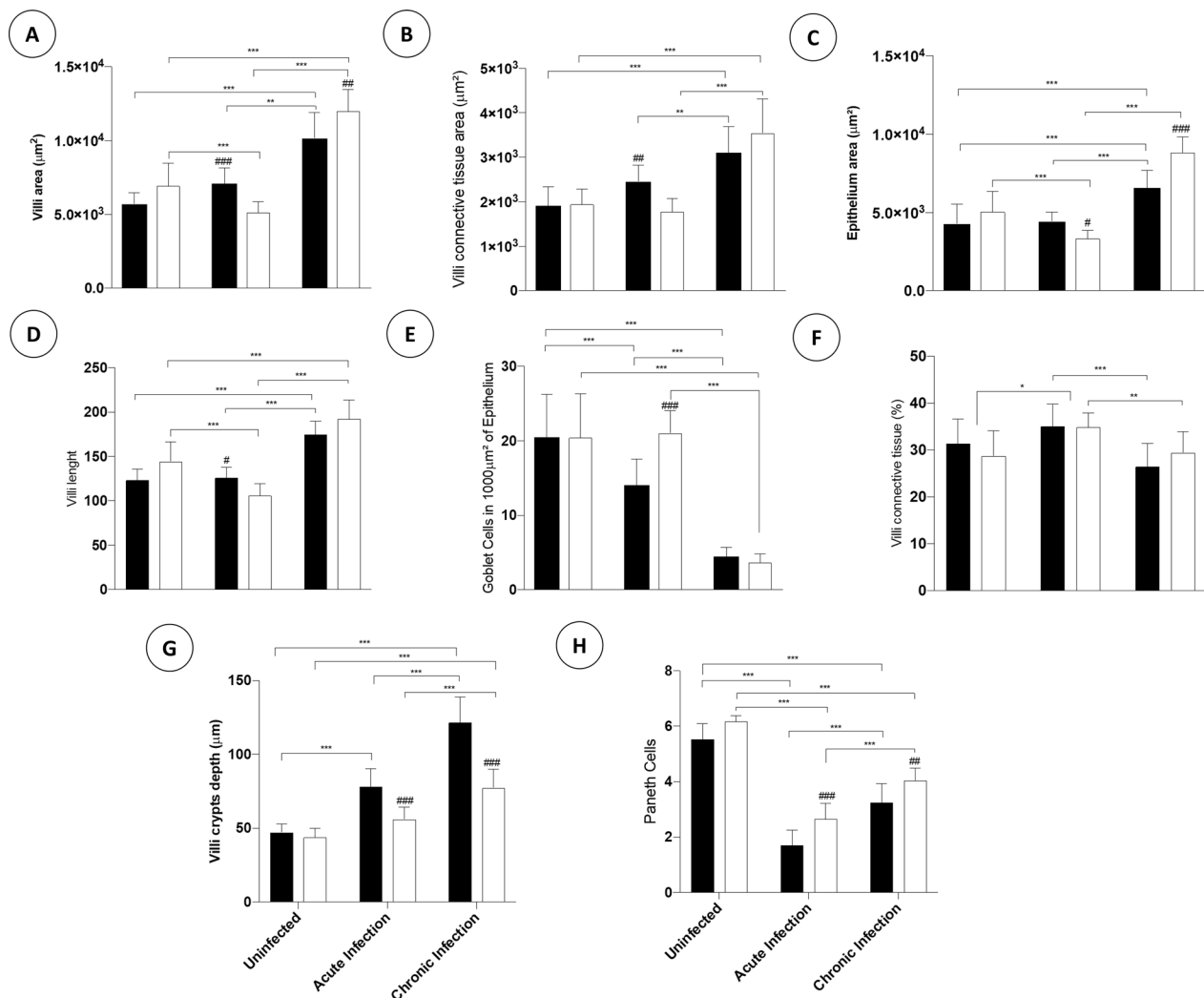


**Fig. 8** Morphometric study of the ileum in C57BL/6 mice, infected or not with *T. gondii* and treated or not with SGE (30  $\mu\text{g}$ ) during the chronic or acute phases. # Represents significant differences between groups in the same phase of the disease. \* Represents differences between different experimental conditions (uninfected, acute infection, and chronic infection). Tests were performed using two-way ANOVA followed by Tukey's multiple comparison post-test, and differences were considered significant when \*  $\leq 0.05$ , \*\*  $\leq 0.01$ , \*\*\*  $\leq 0.001$ . #  $\leq 0.05$ , ##  $\leq 0.01$ , ###  $\leq 0.001$  (n = 10 mice per group)

mice and the acute infection phase. Also, untreated animals had fewer goblet cells in the acute phase than SGE-treated mice. (Fig. 8E).

Regarding the percentage of connective tissue in the villi, the results showed that animals treated with SGE in the acute phase had a higher percentage compared to those treated with the same dose in the chronic phase and uninfected animals. Additionally, chronic phase animals in the acute phase had a higher percentage of connective tissue compared to the chronic phase mice (Fig. 8F). *T. gondii* infection significantly increased crypt depth during the acute phase, with an even more pronounced increase in the chronic phase than in the acute infection

phase. In both the acute and chronic phases, animals treated with SGE had significantly shallower crypts compared to infected, untreated animals (Fig. 8G). *T. gondii* infection reduced the number of Paneth cells during the acute infection phase, followed by a slight recovery in the chronic phase. In the acute and chronic infection phases, animals treated with SGE had more Paneth cells than untreated mice. (Fig. 8H).

Histologically, uninfected animals maintained preserved intestinal morphology. In the acute phase, untreated animals showed a marked increase in crypt depth, subepithelial edema, and increased connective tissue and epithelial area (due to cellular hypertrophy), as

well as increased villus area and length (due to a combination of excess connective tissue and inflammatory tissue hypertrophy). In contrast, animals treated with SGE showed less edema, reduced crypt depth, and fewer immunopathological alterations (Fig. 9A–D).

In the chronic phase, untreated animals exhibited extensive subepithelial edema and deep crypts. However, animals treated with SGE showed better epithelial recovery, reduced edema, and larger villi than untreated animals (Figs 9E–H). Regarding Paneth cells, image analysis revealed that uninfected groups maintained these cells. Infected animals in the acute phase

had a depletion of Paneth cells. However, treatment with SGE in either the acute or chronic phase resulted in a significant increase in the number of these cells compared to untreated groups (Fig. 10). In conclusion, treatment with SGE positively impacted intestinal morphology recovery in infected mice, particularly in the chronic phase. There was a significant increase in villus area, connective tissue, epithelium, and villus length in animals treated with SGE during the chronic phase, suggesting a protective and regenerative effect of SGE on the intestinal mucosa.

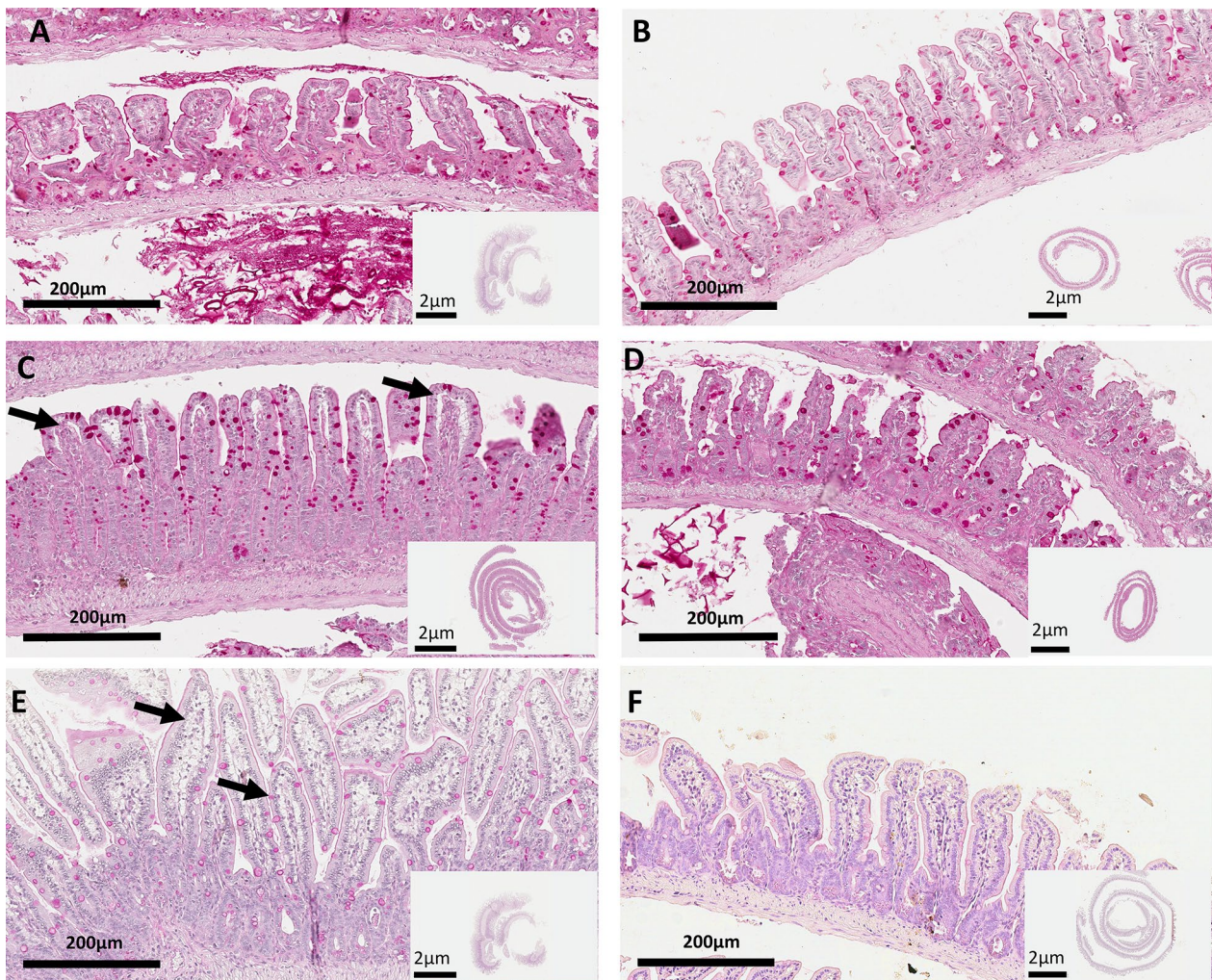


**Fig. 9** Ileum of C57BL/6 mice, infected or not with *T. gondii* and treated or not with SGE 30 µg during the chronic or acute phases. Tissue sections of 4 µm, embedded in paraffin, were stained with Periodic Acid-Schiff (PAS). The slides were scanned, and images were captured using Aperio Imagescope software (version 12.3.3). Original magnification: 20x. Arrows indicate subepithelial edema. The scale bar represents 200 µm for a 20 × magnification of the epithelium or 2 µm for a 2 × magnification of a Swiss roll. The categories represented are: **A** Uninfected, untreated animals; **B** Uninfected animals treated with SGE 30 µg; **C** Infected, untreated animals in the acute phase; **D** Infected animals treated with SGE 30 µg in the acute phase; **E** Infected, untreated animals in the chronic phase; **F** Infected animals treated with SGE 30 µg in the chronic phase

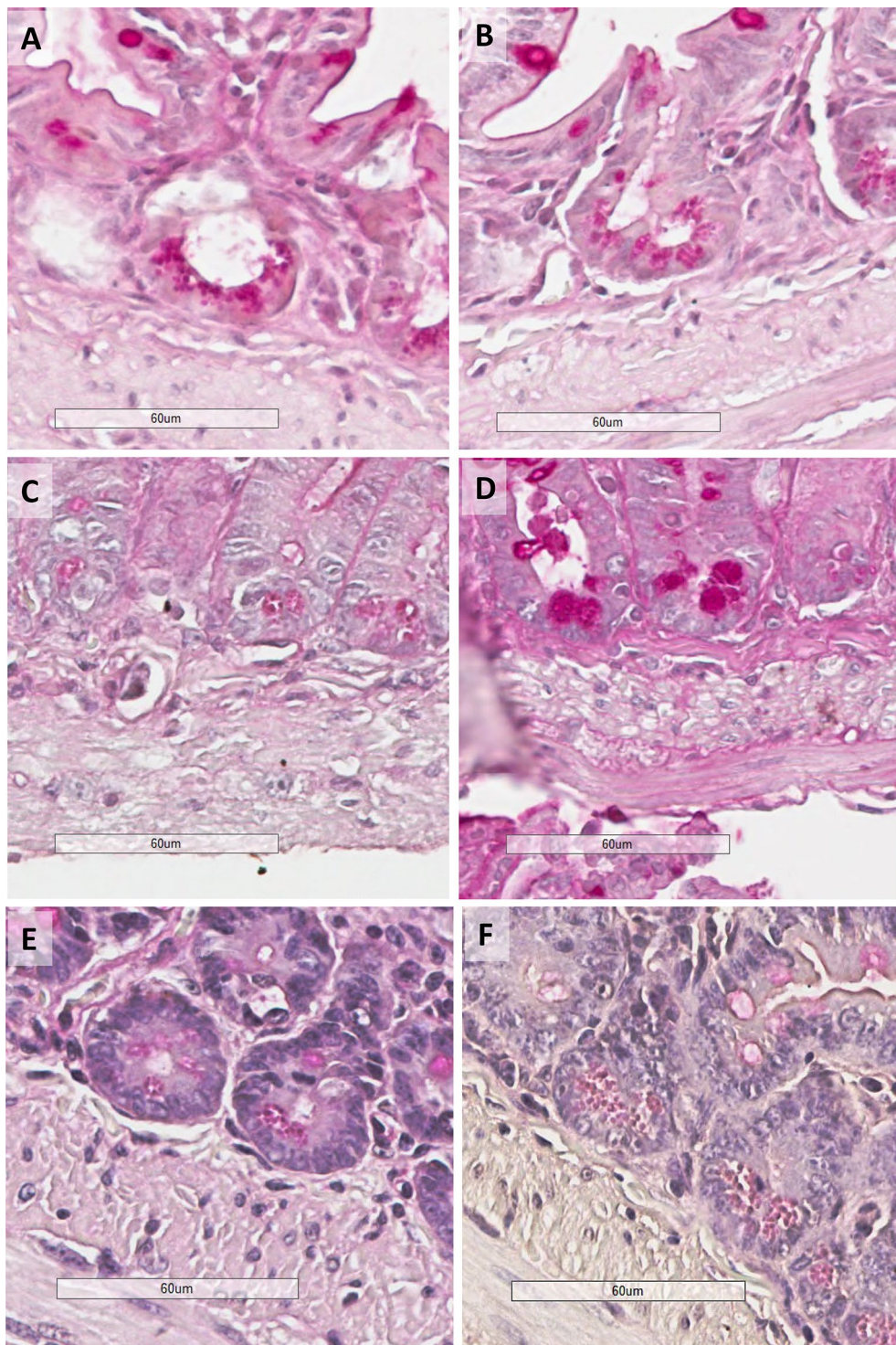


**Fig. 10** Paneth cells in the ileum of C57BL/6 mice, infected or not with *T. gondii* and treated or not with SGE 30 μg during the chronic or acute phases. Tissue sections of 4 μm, embedded in paraffin, were stained with Periodic Acid-Schiff (PAS). The slides were scanned, and images were captured using Aperio Imagescope software (version 12.3.3). Original magnification: 40x. Scale bar = 60 μm. The categories represented are: **A** Uninfected, untreated animals; **B** Uninfected animals treated with SGE 30 μg; **C** Infected, untreated animals in the acute phase; **D** Infected animals treated with SGE 30 μg in the acute phase; **E** Infected, untreated animals in the chronic phase; **F** Infected animals treated with SGE 30 μg in the chronic phase

### SGE alters disease correlation patterns throughout the disease phases

In the acute phase of *T. gondii* infection, untreated animals exhibited strong positive correlations between the duodenal and ileal villi area and their epithelial layers, indicating a consistent growth pattern within the intestines. Similarly, serum IL-2 and IL-17 levels correlated positively, suggesting a coordinated immune response. Conversely, IL-10 showed negative correlations with IL-4 and IL-17, reflecting an antagonistic relationship in regulating inflammation (Figs 11A and 12A).

In animals treated with SGE, strong correlations between villi and epithelial areas in the ileum were noted, indicating that the treatment helps maintain mucosal structure. Cytokines such as IL-10 and IL-17 demonstrated high positive correlations, suggesting effective immune modulation by the treatment. Additionally, significant correlations were observed between serum IL-4 and both IL-10 and IL-17, while a negative correlation was noted between IL-2 and Paneth cell numbers, potentially indicating impacts on intestinal barrier function (Figs 11B and 12B).

During the chronic phase, untreated animals showed that IL-10 was negatively correlated with pro-inflammatory cytokines like IFN- $\gamma$  and TNF, suggesting its role in limiting inflammation. Pro-inflammatory cytokines, including IFN- $\gamma$  and IL-17, demonstrated high correlations with goblet cell numbers and between intestinal IFN- $\gamma$  and IL-22, indicating a coordinated immune response aimed at inflammation and repair. Negative correlations between weight loss and cytokines such as IL-17 and TNF suggested that intense inflammatory responses may impair nutrient absorption and contribute to weight loss (Figs 11C and 12C).

For animals treated with 30  $\mu\text{g}$  of SGE during the chronic phase, high correlations between serum IL-4, IL-6, IL-2, and IL-10 were observed, reflecting a strong interaction among these cytokines and their roles in inflammation and immune regulation. For instance, IL-2 and IL-6 showed a high correlation, indicating their joint involvement in the inflammatory response. TGF- $\beta$  negatively correlated with several ileal tissue parameters and serum IFN- $\gamma$ , suggesting higher TGF- $\beta$  levels are linked to reduced values in these measures. Conversely, TGF- $\beta$  positively correlated with intestinal IFN- $\gamma$  and duodenal tissue areas, suggesting it affects immune response and intestinal structure differently across regions. Overall, the analysis reveals how different cytokines and intestinal parameters interact during *T. gondii* infection, showing patterns of immune response and tissue damage that vary with treatment and infection phases (Figs 11D and 12D).

### Discussion

The intestinal barrier allows water uptake and nutrients while protecting against pathogens. Furthermore, the intestinal barrier must coexist harmoniously with gut microbiota, which plays a key role in host immunology and nutrient metabolism [19, 20]. On the other hand, parasites such as *T. gondii* can challenge the intestinal barrier and disrupt its homeostasis [21]. When C57BL/6 mice are orally infected by *T. gondii*, these mice develop a dysregulated inflammatory process that shares some immunopathological features with Crohn's disease [8]. This inflammatory response promotes lesions in the ileum, and it is primarily orchestrated by Th1 cells, Nitric Oxide (NO), and cytokines, including IL-12, IFN- $\gamma$ , and TNF [22].

It is important to highlight that this study used C57BL/6 mice, a model known for its high susceptibility to *T. gondii* infection. The choice of this model is justified by its relevance in the investigation of the pathogenesis of toxoplasmosis, as the infection in these mice reproduces immunopathological characteristics observed in Crohn's disease in humans. The susceptibility of C57BL/6 mice to ileitis induced by *Toxoplasma gondii* is strongly associated with the activation of the CCR2 chemokine receptor and the immune response mediated by T cells. During infection, CCR2 is essential for the recruitment of CCR2+CD4+T cells to the intestinal lamina propria, where they interact with intraepithelial T cells (IELs), exacerbating inflammation. Additionally, the signaling of Th1 cytokines, such as TNF- $\alpha$ , plays a central role in pathogenesis, similar to what is observed in Crohn's disease. The elevated presence of CCR2 and its ligands, along with an increase in gram-negative bacteria in the gut, contributes to transmural damage and inflammation characteristic of ileitis. These immune and inflammatory interactions make C57BL/6 mice more susceptible to developing intestinal lesions when infected with *T. gondii*, with the presence of T cells and IELs further promoting the pro-inflammatory pathology [8, 23, 24]. In contrast, *R. prolixus* saliva contains various substances, like lipocalins, apyrases, and nitrophorins, which can induce a regulatory immune response [11]. Therefore, we aimed to explore the immunomodulatory effects of *R. prolixus* SGE during the dysregulated inflammatory processes induced by *T. gondii* in C57BL/6 mice. To assess the effectiveness of SGE in mitigating the deleterious effects of toxoplasmosis, we evaluated survival rates, clinical scores, weight loss, and small intestine length. Our data revealed that animals treated with 30  $\mu\text{g}$  of SGE exhibited improved clinical parameters. In contrast, animals treated with 10  $\mu\text{g}$  of SGE did not elicit a strong systemic protective response.

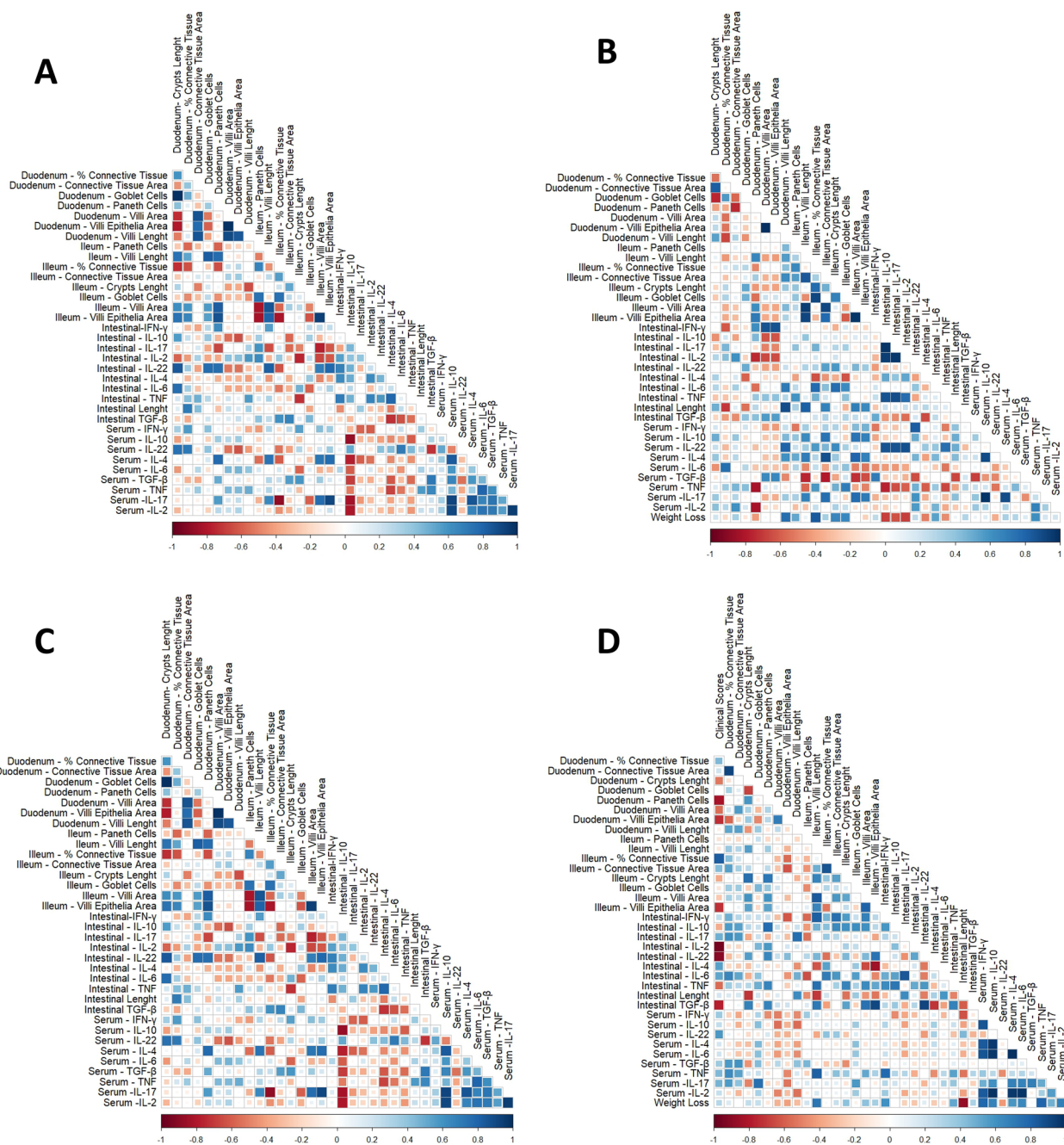


**Fig. 11** Heatmaps illustrating the correlation matrices associated with disease immunopathology, highlighting the relationships between the different parameters analyzed. C57BL/6 mice, infected or not with *T. gondii* and treated or not with SGE 30 µg during the acute and chronic phases. Correlation matrices were calculated using R Studio software, employing the Spearman test for non-parametric samples and the Pearson test for parametric samples. Heatmaps were then generated using the "corrplot" package. Correlations are represented by colors: red indicates negative correlations and blue indicates positive correlations, with color intensity reflecting the strength of the correlation. The categories analyzed are: **A** infected and untreated animals in the acute phase; **B** infected animals treated with SGE 30 µg in the acute phase; **C** infected and untreated animals in the chronic phase; and **D** infected animals treated with SGE 30 µg in the chronic phase

We hypothesized that 30 µg of SGE enhances the regulatory response during infection, thereby mitigating the harmful effects of an uncontrolled immune response. It is

well-established that an intact intestinal barrier protects the host and prevents diseases [25]. In C57BL/6 mice, an impaired immune response can result in the destruction



during the chronic phase of infection, we have observed a decrease in both serum and intestinal levels of this cytokine, which could be attributed to successful infection control. *T. gondii* infection triggers a powerful cell-mediated immune response in which IFN- $\gamma$  plays a central role. Furthermore, this cytokine is essential for mediating *T. gondii* killing inside the parasitophorous vacuole [27].

Our data showed that, during the acute phase, treated animals exhibited significantly higher levels of systemic TNF compared to non-treated mice. TNF plays a pivotal role in immunopathology but is also crucial for combating the parasite. On the other hand, activation of the two TNF receptors (TNFRs) can mediate cell survival through the activation of the classical and alternative NF $\kappa$ B (Nuclear Factor kappa-light-chain-enhancer of activated B cells) pathways, as well as MAP kinase pathways [28, 29]. It is well-known that *T. gondii* infection initially triggers IL-12, which synergistically acts with TNF to stimulate the production of IFN- $\gamma$  by NK cells. This coordinated immune response is essential for effective defense against *T. gondii* infection [30]. Furthermore, our data have demonstrated a significant increase in the levels of IL-12 in the small intestine of treated animals during the acute phase compared to non-infected mice infected with *T. gondii*.

MIF is an important cytokine that acts as a regulator of both innate and adaptive immune responses, playing a crucial role in the protection against *T. gondii* [31–34]. Our findings reveal elevated serum MIF levels during the chronic infection phase, indicative of a potential protective response aimed at controlling the parasite and facilitating tissue repair. This surge in MIF levels may be linked to its recognized capacity for angiogenesis and cellular proliferation [35]. Our data demonstrate that intestinal MIF increases in the acute infection phase and decreases in the chronic phase. The intestine serves as the primary inflammatory focus promoted by *T. gondii* and is crucial for controlling the infection. Furthermore, the reduction of MIF in the chronic infection phase may result in increased activity of regulatory cytokines, facilitating tissue repair and regeneration. Mice deficient in MIF and infected with *T. gondii* displayed heightened pathology and a significantly higher mortality rate than WT mice [36].

Furthermore, our data demonstrated that mice treated with SGE displayed an up-regulation of systemic IL-17 during the chronic phase, showing significantly higher levels compared to both the treated uninfected and treated acute phase groups. IL-17 is a proinflammatory cytokine that plays a crucial role in generating an optimal polymorphonuclear defense against *T. gondii*. IL-17 knockout mice exhibited increased mortality, which

can be attributed to a defect in the migration of polymorphonuclear leukocytes to infected sites during the early stages of infection [37]. We suggest that IL-17 is involved in tissue repair and homeostasis. During the chronic infection phase, as the host attempts to control the infection and repair damaged tissues, the upregulation of IL-17 may be part of the immune system's efforts to restore normal tissue function [38].

Moreover, our results showed that *T. gondii* infection increased the production of serum and intestinal IL-6 both during the chronic and acute infection phases. Studies have suggested that in the absence of IL-6, mice are unable to initiate a rapid proinflammatory response against *T. gondii*, which allows for increased parasite growth. We propose that the presence of IL-6 is crucial for combating the parasite and effectively controlling the infection [39]. SGE-treated animals have presented significantly more intestinal IL-22 in the acute phase and more peripheral blood IL-22 in the chronic phase than to non-treated groups. IL-22 plays a pivotal role in the defense against pathogens due to its ability to promote wound healing, tissue repair, mucus production, and the production of antimicrobial proteins (AMPs) [40]. We have proposed that SGE could positively modulate the secretion of IL-22, thereby attenuating intestinal damage and facilitating tissue repair. Consequently, this modulation may lead to a more preserved intestinal environment. Additionally, IL-22 promotes the production of mucin, which acts as a protective barrier, preventing the direct invasion of bacteria into the intestinal epithelial cells [41].

A previous study has indicated that IL-23 plays a role in the development of intestinal immunopathology in response to *T. gondii* and in a model of inflammatory bowel disease [42]. Our findings revealed that during the acute phase, animals treated with SGE exhibited reduced intestinal IL-23 compared to the non-treated group, which may be associated with better morbidity score data in the treated group. On the other hand, in the chronic infection phase, the treated group showed a significant increase in intestinal IL-23 compared to the non-treated group. During the chronic phase, when the intestine is not the focus of infection, intestinal IL-23 may perform an alternative role. Recent studies have provided evidence that administering exogenous IL-23 can effectively restore IL-22 production and facilitate gut recovery. Furthermore, these studies have demonstrated the existence of a cytokine network involving IL-36 $\gamma$ , IL-23, and IL-22. This network plays a critical role in promoting antimicrobial activity, facilitating tissue repair, and supporting overall host survival [43].

During the chronic infection phase, SGE treatment has led to an increase in serum IL-10 and IL-4 levels. During

infection, IL-10 exerts inhibitory effects on Th1 cells, NK cells, and macrophages, crucial for efficient pathogen clearance. However, excessive activation of these cells can also result in tissue damage. Therefore, IL-10 plays a dual role: it dampens the immune response to prevent excessive inflammation and tissue damage while maintaining a balance to support optimal pathogen clearance. IL-4 is another important cytokine due to its ability to control inflammation and down-regulate Th1 cytokines. Studies have shown that mice deficient in IL-4 or IL-10 exhibit higher mortality and increased pathology. Additionally, these studies have found significantly greater numbers of *T. gondii* cysts in the brains of IL-4 knockout mice than to wild-type [44]. SGE treatment increased intestinal IL-2 during the acute infection phase and serum IL-2 during the chronic phase. Studies have highlighted the critical role of IL-2 in maintaining Foxp3+ regulatory T cells (Treg cells). In the absence of IL-2, there is a significant depletion of Treg cells, leading to a severe deficiency that can contribute to the development of autoimmune disorders [45].

Our data demonstrated that intestinal IL-5 is predominantly produced during the acute infection phase compared to the chronic phase. Studies suggest that IL-5 may play a role in the production of IL-12. Additionally, IL-5 exerts pleiotropic activities on various target cells, including B cells, eosinophils, and basophils. It is produced by both hematopoietic and non-hematopoietic cells, including T cells, granulocytes, and natural helper cells [46]. Along these lines, we suggest that IL-5 plays an important role in the immune response against *T. gondii* during the acute phase. The present study showed that intestinal TGF- $\beta$  is predominantly produced during acute infection, while serum TGF- $\beta$  is more prominent during chronic infection. TGF- $\beta$  is a potent immunosuppressive cytokine that plays a crucial role in developing and regulating various immune cells [47]. Nevertheless, it is known that TGF- $\beta$  plays a dual role in *T. gondii* infection. In collaboration with IL-6 and IL-23, TGF- $\beta$  promotes the production of IL-17 by NK cells and contributes to the development of Th17 lymphocytes during toxoplasmosis. This coordinated immune response is essential for parasite control [48].

In the acute phase of infection, administration of SGE has demonstrated a positive impact on the morphometric parameters of the ileum in treated animals. Treatment with SGE led to significant improvements in intestinal health. Specifically, in the acute phase, SGE reduced edema, crypt depth, and immunopathological changes while increasing the number of Paneth cells, essential for intestinal defense. In the chronic phase, SGE continued to promote recovery in the ileum, with reduced edema, increased villus size, and a higher number of

Paneth cells than untreated animals. The protective effects also extended to the duodenum, where SGE treatment improved villus size, reduced crypt depth, and increased the number of goblet and Paneth cells, aiding in the recovery of intestinal architecture and function. In C57BL/6 mice, death typically occurs between 7 and 10 days after infection, accompanied by extensive necrosis of villi and mucosal cells in the ileum of the small intestine. This necrotic process leads to the destruction of the villi and the subsequent shortening of these structures [6, 22]. Necrosis depends on CD4+ T lymphocytes, IFN- $\gamma$ , and nitric oxide, as demonstrated in previous studies [49, 50]. Additionally, the original study revealed that damage induction was mediated by  $\alpha\beta$ TCR+ cells but not by  $\gamma\delta$ TCR+ cells [6].

During inflammation, the connective tissue of the villi can undergo several alterations that impact its function. Increased blood vessel permeability leads to edema, while fibroblast hyperplasia and excessive collagen fiber production contribute to fibrosis and tissue thickening, impairing nutrient absorption. Additionally, the infiltration of immune cells and modifications in the extracellular matrix may further damage the tissue, compromising villus function. These changes can worsen inflammatory conditions and negatively affect intestinal health [51, 52]. Along these lines, we hypothesize that the immunoregulatory effects of SGE are responsible for mitigating the detrimental effects observed in infected animals. Infected and untreated animals during the acute phase exhibit increased deposition of connective tissue in the ileum, which correlates with a reduced intestinal epithelium. This is associated with heightened edema, inflammation, and ongoing attempts at tissue repair. The increased connective tissue indicates a robust inflammatory response, as well as the body's efforts to restore the damaged intestinal mucosa. Connective tissue plays a critical role in repairing the intestinal epithelium after injury. When the epithelium is damaged, the lamina propria, a connective tissue layer beneath the epithelium, is activated to initiate the healing process. Fibroblasts, which are responsible for producing the extracellular matrix, proliferate and generate new collagen fibers and other matrix components. This newly formed matrix provides structural support necessary for epithelial cell regeneration and the restoration of mucosal integrity [53, 54].

We observed an increase in the size and area of villi in the duodenum of treated animals during the chronic phase. Similarly, in the ileum, both treated and untreated groups showed an increase in villus size during the chronic phase. *T. gondii* infection may lead to a persistent enlargement of intestinal villi, both in the duodenum and ileum, during the chronic phase. This response could be attributed to chronic inflammation, tissue remodeling,

changes in the microbiota, and immune mechanisms. These processes likely represent the organism's attempt to compensate for damage and maintain nutrient absorption [55]. In treated groups, the positive regulation of cytokines such as IL-22, IL-4, IL-10, and TGF- $\beta$  during the chronic phase can significantly influence cell proliferation and the differentiation of stem cells in the intestinal crypts. These cytokines play pivotal roles in regulating the inflammatory environment and maintaining intestinal homeostasis, directly impacting the renewal and function of epithelial stem cells. For instance, IL-22 and TGF- $\beta$  are recognized for their ability to modulate both intestinal regeneration and the inflammatory response, thereby affecting the dynamics of stem cells in the intestinal crypts [41, 56–58]

During the inflammatory and destructive processes affecting intestinal villi, the body initiates a repair mechanism to restore tissue integrity. Crypts, which are glandular structures located at the base of the villi, contain intestinal stem cells responsible for epithelial renewal. In response to inflammation, these stem cells are activated to proliferate and differentiate into new epithelial cells. These newly formed cells then migrate from the base to the tip of the villi to replace damaged cells. The increased proliferative activity leads to an enlargement of the crypts, reflecting the body's need for accelerated cell production to repair the injured tissue [59]. Inflammation can induce changes in intestinal tissue architecture, including the remodeling of crypts. This process often involves alterations in the size and shape of the crypts, leading to their expansion. The infiltration of immune cells during inflammation also plays a key role, as these cells release signaling molecules that stimulate the proliferation of crypt cells, further promoting their growth. Together, these mechanisms facilitate a rapid and effective response to repair tissue damage caused by inflammation, helping restore intestinal function [60, 61]. In this context, untreated animals typically exhibit larger crypts, reflecting more significant damage to the intestinal barrier and a more intense inflammatory response. As a result, there is an increased in stem cells proliferation to compensate for the extensive tissue damage.

Our results demonstrated that both in the ileum and the duodenum, animals treated with SGE showed an increase in the number of goblet cells. In the context of *T. gondii* infection, goblet cells play a crucial role in the host's defense. The mucus secreted by these cells acts as a physical barrier, preventing the adhesion and penetration of the parasite into the intestinal mucosa. Additionally, mucus contains antimicrobial molecules, such as immunoglobulins, antimicrobial peptides, and enzymes, which contributes to the control of *T. gondii* proliferation. Studies also suggest that goblet cells participate in

the immune response against the parasite by modulating the activity of immune cells and secreting pro-inflammatory cytokines. In this context, a higher number of goblet cells may be associated with reduced parasitism during the chronic phase of infection [62, 63].

Our results highlighted a significant reduction in the number of goblet cells in animals during the chronic phase. Oral infection with *T. gondii* can lead to a marked decrease in goblet cell numbers due to a combination of factors. The inflammatory response triggered by the infection, similar to what occurs in chronic inflammations such as inflammatory bowel diseases, can directly damage these cells or disrupt the intestinal microenvironment, impairing their survival and differentiation. Furthermore, the parasite may alter the intestinal microbiota, affect cellular signaling pathways involved in goblet cell differentiation, and modulate the immune response in the mucosa, indirectly impacting goblet cell population dynamics [21]. In the context of SGE treatment, the observed increase in the number of goblet cells, particularly in the duodenum during the chronic phase, underscores its positive impact on intestinal protection and regeneration. This finding suggests that SGE plays a crucial role in maintaining the integrity of the intestinal mucosa by promoting the proliferation of goblet cells and enhancing mucus production, which is essential for defense against pathogens. Furthermore, the increase in goblet cells may indicate an effective repair process and a strengthening of the mucosal barrier function [21, 62].

The SGE from various species of triatomines exhibits immunomodulatory potential, influencing the immune response in distinct ways. In vitro studies demonstrated that the SGE from *P. lignarius*, *M. pallidipennis*, *T. lecticularia*, and *R. prolixus* inhibited dendritic cell (DC) differentiation and modulated the expression of costimulatory molecules on mature DCs. Additionally, the SGE suppressed the production of pro-inflammatory cytokines while promoting the production of IL-10 in LPS-stimulated DCs. In vivo studies further support the immunomodulatory capacity of SGE in mitigating inflammatory damage. In the DSS-induced colitis model, the SGE from *T. lecticularia* alleviated the severity of intestinal inflammation by reducing levels of the inflammatory cytokine IL-6 and increasing the regulatory cytokine IL-10 in the intestine [9]. It is important to note that the composition of SGE varies across triatomine species, and this variation may account for the differences in the observed effects.

The susceptibility of the C57BL/6 mouse model to *Toxoplasma gondii* infection likely influenced the magnitude of the protective effects observed with SGE treatment at 30  $\mu$ g. The intense intestinal inflammation characteristic of this strain may have amplified the

therapeutic benefits of SGE, underscoring its potential as a modulator of exaggerated inflammatory responses. While the widespread use of the C57BL/6 model in *T. gondii* research facilitates comparative studies, it also limits the generalizability of findings to other strains or to humans. Nonetheless, this model was instrumental in elucidating the immunopathological mechanisms of toxoplasmosis and the effects of SGE in the context of severe inflammation. SGE demonstrated significant protective effects, including reduced weight loss during the chronic phase, preservation of intestinal integrity, and a balanced immune response (Fig. 13). These findings align with the broader immunomodulatory properties of salivary gland extracts SGE from various triatomine species, which influence immune responses and hold therapeutic potential for infectious and inflammatory diseases.

Future research should explore the mechanisms of SGE more comprehensively, examining its impact on immune cell populations, signaling pathways, intestinal microbiota, and gene expression to identify potential therapeutic targets. Moreover, we acknowledge the importance of this analysis for a more comprehensive understanding of the infection, and thus, we plan to include parasite load quantification in our future studies to better correlate the immune effects with parasite burden.

**Declaration of generative AI and AI-assisted technologies in the writing process**

During the preparation of this work the author(s) used ChatGPT 3.5/OpenAI in order to improve readability and language. After using this tool/service, the author(s) reviewed and edited the content as needed and take(s) full responsibility for the content of the publication.

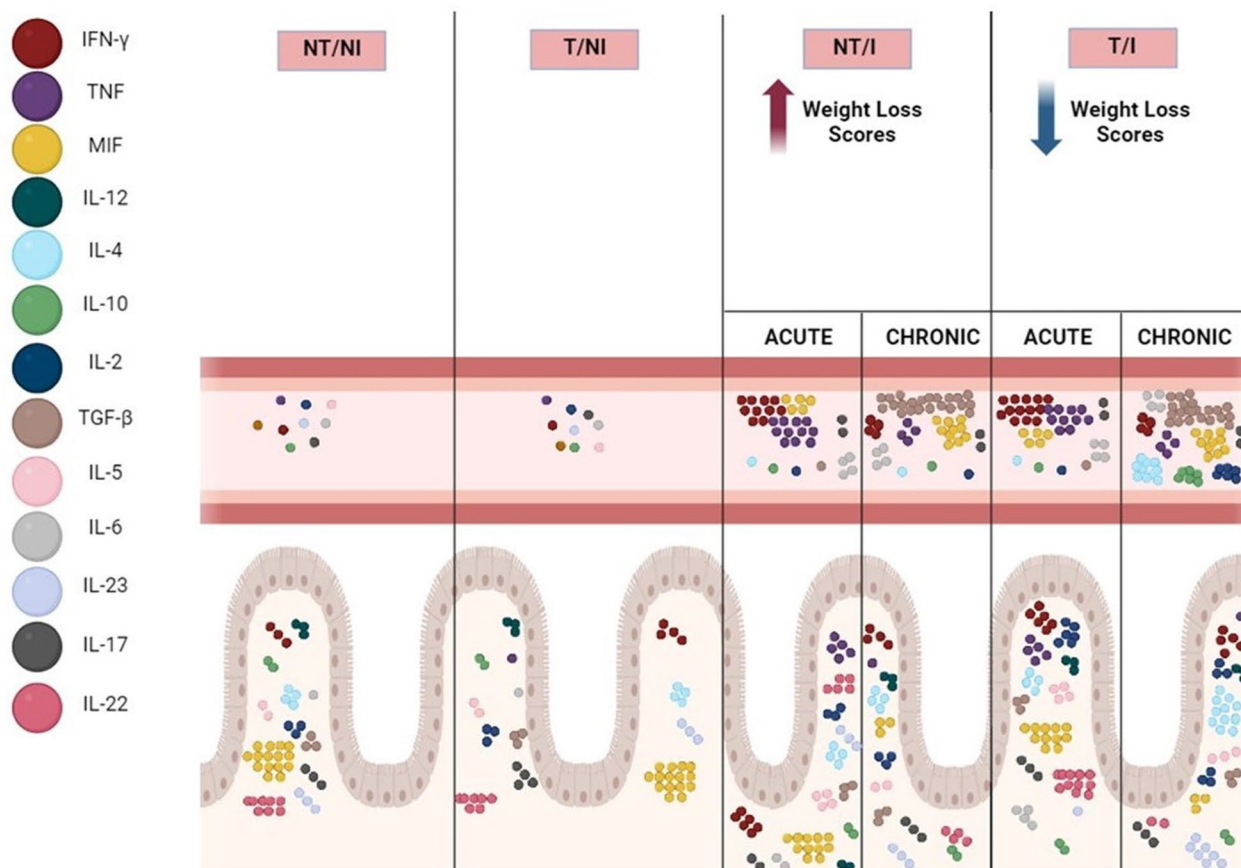


**Fig. 13** Schematic model representing *T. gondii* infection in C57BL/6 mice and the influence of SGE treatment on cytokine release in serum and the small intestine. Our data demonstrate that *T. gondii* infection increases the levels of inflammatory cytokines such as TNF and IFN- $\gamma$  in both mouse serum and small intestine tissue. Additionally, animals treated with the highest concentration of SGE experienced less weight loss and lower clinical scores. Specifically, mice treated with SGE 30  $\mu\text{g}$  exhibited a significant increase in systemic regulatory cytokines, including IL-4, IL-2, and IL-10, during the chronic phase of infection. Cytokine analysis further revealed that SGE-treated mice secreted more intestinal IL-4 in the chronic phase and increased levels of IL-2 and IL-22 in the acute phase. Moreover, cyst counts indicated that SGE-treated groups had significantly fewer cysts in brain tissue compared to the untreated group. Therefore, our findings demonstrate that SGE has the ability to induce a regulatory response, mitigating the detrimental effects of uncontrolled inflammation and providing protection against *T. gondii* infection

### Author contributions

RAPS, JHNP, RJS, SCT, FBFF, AHLG, TGOL, MJG-R, MVS, MLMG and AOG did the experimental design and analysis; RAPS, AHLG, TGOL did graphs and figures; RAPS wrote the main manuscript text; MVS, VRJ, JRM, BFB, EAVF, CJFO, AOG, did analyzed results, revised the manuscript, and added for Funding acquisition and Conceptualization; AOG did Supervision and project administration.

### Funding

The authors thanks the financial support obtained from Brazilian Research Agencies: Conselho Nacional de Pesquisa Científica e Tecnológica (CNPq; 309364/2022-1) and Fundação de Amparo à Pesquisa de Minas Gerais (FAPEMIG).

### Data availability

No datasets were generated or analysed during the current study.

### Declarations

#### Competing interests

The authors declare no competing interests.

#### Author details

<sup>1</sup>Laboratório de Interações Celulares, Instituto de Ciências Biológicas E Naturais, Universidade Federal Do Triângulo Mineiro (UFMTM). Av. Getúlio Guaritá, 159-Nossa Sra. da Abadia, Uberaba, Minas Gerais 38025-440, Brazil. <sup>2</sup>Instituto de Ciências Biomédicas, Universidade Federal de Uberlândia, Uberlândia, Minas Gerais, Brazil.

Received: 10 October 2024 Accepted: 24 December 2024

Published online: 05 March 2025

### References

- Montoya J, Liesenfeld O. *Toxoplasmosis*. Lancet. 2004;363(9425):1965–76. [https://doi.org/10.1016/S0140-6736\(04\)16412-X](https://doi.org/10.1016/S0140-6736(04)16412-X).
- Hunter CA, Sibley LD. Modulation of innate immunity by *Toxoplasma gondii* virulence effectors. Nat Rev Microbiol. 2012;10(11):766–78. <https://doi.org/10.1038/nrmicro2858>.
- Vancamelbeke M, Vermeire S. The intestinal barrier: a fundamental role in health and disease. Expert Rev Gastroenterol Hepatol. 2017;11(9):821–34. <https://doi.org/10.1080/17474124.2017.1343143>.
- Baumgart DC, Carding SR. Inflammatory bowel disease: cause and immunobiology. Lancet. 2007;369(9573):1627–40. [https://doi.org/10.1016/S0140-6736\(07\)60750-8](https://doi.org/10.1016/S0140-6736(07)60750-8).
- Ha F, Khalil H. Crohn's disease: a clinical update. Therap Adv Gastroenterol. 2015;8(6):352–9. <https://doi.org/10.1177/1756283X15592585>.
- Liesenfeld O, Kosek J, Remington JS, Suzuki Y. Association of CD4+ T cell-dependent, interferon-gamma-mediated necrosis of the small intestine with genetic susceptibility of mice to peroral infection with *Toxoplasma gondii*. J Exp Med. 1996;184(2):597–607. <https://doi.org/10.1084/jem.184.2.597>.
- Nagpal R, Yadav H. Bacterial translocation from the gut to the distant organs: an overview. Ann Nutr Metab. 2017;71(Suppl1):11–6. <https://doi.org/10.1159/000479918>.
- Egan CE, Cohen SB, Denkers EY. Insights into inflammatory bowel disease using *Toxoplasma gondii* as an infectious trigger. Immunol Cell Biol. 2012;90(7):668–75. <https://doi.org/10.1038/icb.2011.93>.
- Sales-Campos H, et al. Salivary gland extract of kissing bug, *Triatoma lecticularia*, reduces the severity of intestinal inflammation through the modulation of the local IL-6/IL-10 axis. Mediat Inflamm. 2018;2018:1–9. <https://doi.org/10.1155/2018/1924393>.
- Arcà B, Ribeiro JM. Saliva of hematophagous insects: a multifaceted toolkit. Curr Opin Insect Sci. 2018;29:102–9. <https://doi.org/10.1016/j.cois.2018.07.012>.
- Montfort WR, Weichsel A, Andersen JF. Nitrophorins and related anti-hemostatic lipocalins from *Rhodnius prolixus* and other blood-sucking arthropods. Biochimica Et Biophys Acta BBA Protein Struct Mol Enzymol. 2000;1482(1–2):110–8.
- Santos DV, et al. An updated catalog of lipocalins of the chagas disease vector *Rhodnius prolixus* (Hemiptera, Reduviidae). Insect Biochem Mol Biol. 2022;146:103797. <https://doi.org/10.1016/j.ibmb.2022.103797>.
- Pittman KJ, Knoll LJ. Long-term relationships: the complicated interplay between the host and the developmental stages of *Toxoplasma gondii* during Acute and chronic infections. Microbiol Mol Biol Rev. 2015;79(4):387–401. <https://doi.org/10.1128/MMBR.00027-15>.
- Garfoot AL, Cervantes PW, Knoll LJ. Transcriptional analysis shows a robust host response to *Toxoplasma gondii* during early and late chronic infection in both male and female mice. Infect Immun. 2019;87(5):e00024-e119. <https://doi.org/10.1128/IAI.00024-19>.
- Bartley PM, Wright S, Sales J, Chianini F, Buxton D, Innes EA. Long-term passage of tachyzoites in tissue culture can attenuate virulence of *Neospora caninum* in vivo. Parasitology. 2006. <https://doi.org/10.1017/S0031182006000539>.
- Heimesaat MM, et al. Gram-negative bacteria aggravate murine small intestinal Th1-type immunopathology following oral infection with *Toxoplasma gondii*. J Immunol. 2006;177(12):8785–95. <https://doi.org/10.4049/JIMMUNOL.177.12.8785>.
- Moolenbeek C, Ruitenber EJ. The 'Swiss roll': a simple technique for histological studies of the rodent intestine. Lab Anim. 1981. <https://doi.org/10.1258/002367781780958577>.
- McManus JFA. Histological and histochemical uses of periodic acid. Stain Technol. 1948;23(3):99–108. <https://doi.org/10.3109/10520294809106232>.
- Usuda H, Okamoto T, Wada K. Leaky gut: effect of dietary fiber and fats on microbiome and intestinal barrier. Int J Mol Sci. 2021. <https://doi.org/10.3390/IJMS22147613>.
- Camilleri M, Madsen K, Spiller R, Van Meerveld BG, Verne GN. Intestinal barrier function in health and gastrointestinal disease. Neurogastroenterol Motil. 2012;24(6):503–12. <https://doi.org/10.1111/J.1365-2982.2012.01921.X>.
- Snyder LM, Denkers EY. From initiators to effectors: roadmap through the intestine during encounter of *Toxoplasma gondii* with the mucosal immune system. Front Cell Infect Microbiol. 2021;10: 614701. <https://doi.org/10.3389/FCIMB.2020.614701/BIBTEX>.
- Schreiner M, Liesenfeld O. Small intestinal inflammation following oral infection with *Toxoplasma gondii* does not occur exclusively in C57BL/6 mice: review of 70 reports from the literature. Mem Inst Oswaldo Cruz. 2009;104(2):221–33. <https://doi.org/10.1590/S0074-02762009000200015>.
- Craggs A, Welfare M, Donaldson P, Mansfield J. The CC chemokine receptor 5 Δ32 mutation is not associated with inflammatory bowel disease (IBD) in NE England. Genes Immun. 2001;2(2):114–6. <https://doi.org/10.1038/sj.gene.6363735>.
- Rector A, et al. Analysis of the CC chemokine receptor 5 (CCR5) delta-32 polymorphism in inflammatory bowel disease. Hum Genet. 2001;108(3):190–3. <https://doi.org/10.1007/s004390100462>.
- Di Tommaso N, Gasbarrini A, Ponziani FR. Intestinal barrier in human health and disease. Int J Environ Res Public Health. 2021;18(23):12836. <https://doi.org/10.3390/ijerph182312836>.
- Peuhkuri K. Even low-grade inflammation impacts on small intestinal function. World J Gastroenterol. 2010;16(9):1057. <https://doi.org/10.3748/wjg.v16.i9.1057>.
- Scharton-Kersten TM, et al. In the absence of endogenous IFN-gamma, mice develop unimpaired IL-12 responses to *Toxoplasma gondii* while failing to control acute infection. J Immunol. 1996;157(9):4045–54. <https://doi.org/10.4049/jimmunol.157.9.4045>.
- Chang HR, Grau GE, Pechere JC. Role of TNF and IL-1 in infections with *Toxoplasma gondii*. Immunology. 1990;69:33–7.
- Guicciardi ME, Gores GJ. Life and death by death receptors. FASEB J. 2009;23(6):1625–37. <https://doi.org/10.1096/fj.08-111005>.
- Hunter CA, Subauste CS, Van Cleave VH, Remington JS. Production of gamma interferon by natural killer cells from *Toxoplasma gondii*-infected SCID mice: regulation by interleukin-10, interleukin-12, and tumor necrosis factor alpha. Infect Immun. 1994;62(7):2818–24. <https://doi.org/10.1128/iai.62.7.2818-2824.1994>.
- DE Oliveira Gomes A, et al. Effect of macrophage migration inhibitory factor (MIF) in human placental explants infected with *Toxoplasma gondii*

- depends on gestational age. *Am J Pathol.* 2011;178(6):2792–801. <https://doi.org/10.1016/j.ajpath.2011.02.005>.
32. Gomes AO, et al. Macrophage migration inhibitory factor (MIF) prevents maternal death, but contributes to poor fetal outcome during congenital *Toxoplasmosis*. *Front Microbiol.* 2018. <https://doi.org/10.3389/fmicb.2018.00906>.
  33. Marcon CF, et al. Macrophage migration inhibitory factor (MIF) and pregnancy may impact the balance of intestinal cytokines and the development of intestinal pathology caused by *Toxoplasma gondii* infection. *Cytokine.* 2020;136: 155283. <https://doi.org/10.1016/j.cyto.2020.155283>.
  34. Ferreira PTM, et al. Macrophage migration inhibitory factor contributes to drive phenotypic and functional macrophages activation in response to *Toxoplasma gondii* infection. *Immunobiology.* 2023;228(3): 152357. <https://doi.org/10.1016/j.imbio.2023.152357>.
  35. Ohta S, et al. Macrophage migration inhibitory factor (MIF) promotes cell survival and proliferation of neural stem/progenitor cells. *J Cell Sci.* 2012. <https://doi.org/10.1242/jcs.102210>.
  36. Farr L, et al. CD74 signaling links inflammation to intestinal epithelial cell regeneration and promotes mucosal healing. *Cell Mol Gastroenterol Hepatol.* 2020;10(1):101–12. <https://doi.org/10.1016/j.jcmgh.2020.01.009>.
  37. Zenobia C, Hajishengallis G. Basic biology and role of interleukin-17 in immunity and inflammation. *Periodontol 2000.* 2015;69(1):142–59. <https://doi.org/10.1111/prd.12083>.
  38. Song S, Xiao Z, Dekker FJ, Poelarends GJ, Melgert BN. Macrophage migration inhibitory factor family proteins are multitasking cytokines in tissue injury. *Cell Mol Life Sci.* 2022;79(2):105. <https://doi.org/10.1007/s00018-021-04038-8>.
  39. Passos ST, Silver JS, O'Hara AC, Sehy D, Stumhofer JS, Hunter CA. IL-6 promotes NK cell production of IL-17 during *Toxoplasmosis*. *J Immunol.* 2010;184(4):1776–83. <https://doi.org/10.4049/jimmunol.0901843>.
  40. Keir ME, Yi T, Lu TT, Ghilardi N. The role of IL-22 in intestinal health and disease. *J Exp Med.* 2020. <https://doi.org/10.1084/JEM.20192195>.
  41. Patnaude L, et al. Mechanisms and regulation of IL-22-mediated intestinal epithelial homeostasis and repair. *Life Sci.* 2021;271: 119195. <https://doi.org/10.1016/j.lfs.2021.119195>.
  42. Muñoz M, et al. Interleukin (IL)-23 mediates *Toxoplasma gondii*-induced immunopathology in the gut via matrix metalloproteinase-2 and IL-22 but independent of IL-17. *J Exp Med.* 2009;206(13):3047–59. <https://doi.org/10.1084/jem.20090900>.
  43. Ngo VL, et al. A cytokine network involving IL-36γ, IL-23, and IL-22 promotes antimicrobial defense and recovery from intestinal barrier damage. *Proc Natl Acad Sci.* 2018. <https://doi.org/10.1073/pnas.1718902115>.
  44. Keegan AD, Leonard WJ, Zhu J. Recent advances in understanding the role of IL-4 signaling. *Fac Rev.* 2021. <https://doi.org/10.12703/r/10-71>.
  45. Tchitchek N, et al. Low-dose IL-2 shapes a tolerogenic gut microbiota that improves autoimmunity and gut inflammation. *JCI Insight.* 2022. <https://doi.org/10.1172/jci.insight.159406>.
  46. Takatsu K. Interleukin-5 and IL-5 receptor in health and diseases. *Proceed Jpn Acad Ser B.* 2011;87(8):463–85. <https://doi.org/10.2183/pjab.87.463>.
  47. Kubiczakova L, Sedlarikova L, Hajek R, Sevcikova S. TGF-β – an excellent servant but a bad master. *J Transl Med.* 2012;10(1):183. <https://doi.org/10.1186/1479-5876-10-183>.
  48. Zare-Bidaki M, et al. TGF-β in *Toxoplasmosis*: friend or foe? *Cytokine.* 2016;86:29–35. <https://doi.org/10.1016/j.cyto.2016.07.002>.
  49. Khan IA, Schwartzman JD, Matsuura T, Kasper LH. A dichotomous role for nitric oxide during acute *Toxoplasma gondii* infection in mice. *Proc Natl Acad Sci.* 1997;94(25):13955–60. <https://doi.org/10.1073/pnas.94.25.13955>.
  50. Liesenfeld O, et al. TNF-α, nitric oxide and IFN-γ are all critical for development of necrosis in the small intestine and early mortality in genetically susceptible mice infected perorally with *Toxoplasma gondii*. *Parasite Immunol.* 1999;21(7):365–76. <https://doi.org/10.1046/j.1365-3024.1999.00237.x>.
  51. Dammeier J, Brauchle M, Falk W, Grotendorst GR, Werner S. Connective tissue growth factor: a novel regulator of mucosal repair and fibrosis in inflammatory bowel disease? *Int J Biochem Cell Biol.* 1998;30(8):909–22. [https://doi.org/10.1016/S1357-2725\(98\)00046-6](https://doi.org/10.1016/S1357-2725(98)00046-6).
  52. Shelley-Fraser G, Borley NR, Warren BF, Shepherd NA. The connective tissue changes of Crohn's disease. *Histopathology.* 2012;60(7):1034–44. <https://doi.org/10.1111/j.1365-2559.2011.03911.x>.
  53. Boger KD, Sheridan AE, Ziegler AL, Bliklager AT. Mechanisms and modeling of wound repair in the intestinal epithelium. *Tissue Barriers.* 2023. <https://doi.org/10.1080/21688370.2022.2087454>.
  54. Chalkidi N, Paraskeva C, Koliaraki V. Fibroblasts in intestinal homeostasis, damage, and repair. *Front Immunol.* 2022. <https://doi.org/10.3389/fimmu.2022.924866>.
  55. Tilson MD. Compensatory hypertrophy of the ileum after gastroduodenal exclusion. *Arch Surg.* 1975;110(3):309. <https://doi.org/10.1001/archsurg.1975.01360090079016>.
  56. Beck PL, Rosenberg IM, Xavier RJ, Koh T, Wong JF, Podolsky DK. Transforming growth factor-β mediates intestinal healing and susceptibility to injury in vitro and in vivo through epithelial cells. *Am J Pathol.* 2003;162(2):597–608. [https://doi.org/10.1016/S0002-9440\(10\)63853-9](https://doi.org/10.1016/S0002-9440(10)63853-9).
  57. Nguyen HD, Aljamaei HM, Stadnyk AW. The production and function of endogenous interleukin-10 in intestinal epithelial cells and gut homeostasis. *Cell Mol Gastroenterol Hepatol.* 2021;12(4):1343–52. <https://doi.org/10.1016/j.jcmgh.2021.07.005>.
  58. West G, Matsuura T, Levine A, Klein J, Fiocchi C. Interleukin 4 in inflammatory bowel disease and mucosal immune reactivity. *Gastroenterology.* 1996;110(6):1683–95. <https://doi.org/10.1053/gast.1996.v110.pm8964392>.
  59. Bloemendaal ALA, Buchs NC, George BD, Guy RJ. Intestinal stem cells and intestinal homeostasis in health and in inflammation: a review. *Surgery.* 2016;159(5):1237–48. <https://doi.org/10.1016/j.surg.2016.01.014>.
  60. Asfaha S. Intestinal stem cells and inflammation. *Curr Opin Pharmacol.* 2015;25:62–6. <https://doi.org/10.1016/j.coph.2015.11.008>.
  61. Gersemann M, Stange EF, Wehkamp J. From intestinal stem cells to inflammatory bowel diseases. *World J Gastroenterol.* 2011;17(27):3198–203. <https://doi.org/10.3748/wjg.v17.i27.3198>.
  62. Kim J, Khan W. Goblet cells and mucins: role in innate defense in enteric infections. *Pathogens.* 2013;2(1):55–70. <https://doi.org/10.3390/pathogens2010055>.
  63. McGuckin MA, Hasnain SZ. Goblet cells as mucosal sentinels for immunity. *Mucosal Immunol.* 2017;10(5):1118–21. <https://doi.org/10.1038/mi.2016.132>.

## Publisher's Note

Springer Nature remains neutral with regard to jurisdictional claims in published maps and institutional affiliations.